CATALYTIC COMBUSTION OF METHANOL ON STRUCTURED CATALYSTS FOR DIRECT METHANOL FUEL CELL

A Thesis Submitted to
The Graduate School of Engineering and Sciences of
İzmir Institute of Technology
in Partial Fulfillment of the Requirements for the Degree of

MASTER OF SCIENCE

in Energy Engineering

by
Emel DÖNMEZ

July 2011
İZMİR

We approve the thesis of **Emel DÖNMEZ**

_____
Assoc. Prof. Erol ŞEKER
Supervisor

_____
Assoc. Prof. Gülden GÖKÇEN
Co-Supervisor

_____
Assoc. Prof. Fehime ÖZKAN
Committee Member

_____
Assoc. Prof. Oğuz BAYRAKTAR
Committee Member

_____
Prof. Dr. Levent ARTOK
Committee Member

_____
Asist. Prof. Ekrem ÖZDEMİR
Committee Member

4 July 2011

_____
Assoc. Prof. Gülden GÖKÇEN
Head of the Department of
Energy Engineering

_____
Prof. Dr. Durmuş Ali DEMİR
Dean of the Graduate School of
Engineering and Sciences

ACKNOWLEDGEMENTS

I would like to thank to my MSc supervisor Assoc. Prof. Erol Şeker and MSc co-supervisor Assoc. Prof. Gülden Gökçen for their encouragement, guidance, patience and immense knowledge.

I wish to thank Emrah Önder for helping me get through the difficult times and supporting me a lot throughout the study.

I am grateful to my housemate, Manolya Tan, for her moral support and doing housework for me when I was busy with my study.

I express my thanks to all my friends and colleagues; Selcan Ateş, Burcu Köseoğlu, Mert Tunçer, Selahattin Umdu, Emre Kılıç for their help and friendship.

Finally, most importantly, my special thanks go to my parents and sisters for supporting me spiritually throughout my life.

ABSTRACT

CATALYTIC COMBUSTION OF METHANOL ON STRUCTURED CATALYSTS FOR DIRECT METHANOL FUEL CELL

The major goal of this study is to investigate the effect of metal loading, space velocity and the outside temperature on both the steady state temperature of the alumina supported platinum catalysts and on time to reach at the temperature of 60 ^{o}C of a typical direct methanol fuel cell operating temperature in methanol combustion reaction. Alumina supported platinum catalysts were synthesized by using impregnation method and sol-gel made alumina. The methanol combustion reaction was performed in a tubular reactor.

The characterization of the catalysts was performed by XRD and BET techniques. Particle size of Pt and surface area of the catalysts were compared before and after the reaction.

In this study, it was found that the pure alumina was not active in methanol combustion whereas Pt/Al_2O_3 catalysts with varying loadings were active starting at room temperature. 2, 3 and 5% Pt loading catalysts showed the similar activity so it is possible that the average crystallite size and the crystallite size distribution of Pt on these catalysts would be similar.

The space velocity tests indicated that low space velocity is required to quickly reach at 60 ^{o}C and also to achieve the highest steady state temperature for fresh catalyst whereas high space velocity is required to quickly reach at 60 ^{o}C and to achieve the highest steady state temperature for reused catalyst.

The activity of the catalyst was also tested at sub-room temperatures. It was observed that the steady state temperature of the catalyst decreased and the time to reach at 60 ^{o}C increased when the outside temperature was below the room temperature.

In addition to the tubular reactor, plate reactor was prepared for the methanol combustion. For this purpose, varying concentration alumina sols were coated on the stainless steel plates. However, optimum coating thickness could not be obtained because of the crack formation and peeling offs; thus, further detailed studies are necessary for obtaining stable coating suitable for the catalytic combustion.

ÖZET

DİREKT METANOL YAKIT PİLLERİ İÇİN METANOLÜN YAPISAL KATALİZÖRLER ÜZERİNDE KATALİTİK YANMASI

Bu çalışmada alümina destekli platinyum katalizörler üzerinde metanolün yanma reaksiyonu incelenmiştir. Çalışmanın amacı; metal yüklemenin, alan hızının ve ortam sıcaklığının, hem denge sıcaklığı hem de direkt metanol yakıt pilinin tipik çalışma sıcaklığı olan 60 ^{o}C'ye ulaşma zamanı üzerindeki etkisini incelemektir. Alümina sol-gel yöntemi ile hazırlamış ve platinyum alümina üzerine impregne edilmiştir. Metanol yanma reaksiyonu tübüler reaktörde gerçekleştirilmiştir.

Katalizörlerin karakterizasyonları XRD ve BET analizleri ile yapılmıştır. Reaksiyondan önceki Pt parçacık boyutu ve katalizörlerin yüzey alanları, reaksiyondan sonra yapılan analiz sonuçları ile karşılaştırılmıştır.

Bu çalışmada saf alüminanın metanolün yanma reaksiyonunda aktif olmadığı ancak faklı yüklemelerdeki Pt/Al_2O_3 katalizörlerinin oda sıcaklığında aktif olduğu gözlenmiştir. 2, 3 ve 5% Pt yüklemeli katalizörler benzer aktiviteyi göstermiştir. Bu sonuç platinyumun ortalama kristalit boyutunun ve dağılımının bu yüklemedeki katalizörlerde benzer olduğunu gösterebilir.

En yüksek denge sıcaklığı ve 60 ^{o}C'ye ulaşmak için geçen en düşük zaman, aktive edilmiş katalizörde düşük alan hızına aitken, aktive edilmeden kullanılan katalizörde yüksek alan hızına aittir.

Katalizörlerin aktivitesi oda sıcaklığından daha düşük sıcaklıklarda da test edilmiştir. Ortam sıcaklığı oda sıcaklığından daha düşük olduğunda, katalizörlerin denge sıcaklığının düştüğü ve yeterli sıcaklığa ulaşmak için geçen zamanın yükseldiği gözlenmiştir.

Metanol yanma reaksiyonu için tübüler reaktöre ek olarak, levha reaktör hazırlanmıştır. Bu amaçla, farklı konsantrasyonlarda alümina solleri hazırlanmış ve paslanmaz çelik levhalar üzerine kaplanmıştır. Fakat, kalkmalar ve çatlamalar nedeniyle optimum bir kaplama kalınlığı elde edilememiştir, bu nedenle bu alanda daha fazla çalışma yapılması gerekmektedir.

TABLE OF CONTENTS

LIST OF FIGURES

Figure **Page**

LIST OF TABLES

Table **Page**

CHAPTER 1

INTRODUCTION

Energy plays a pivotal role on the development of the countries in the world. In fact, the level of the development is measured by the amount of energy consumed in a country. According to the International Energy Outlook (IEO), total energy consumption in the world is projected to grow 44% in the period from 2006 to 2030 with an average annual increase of 1.6% (IEO, 2009). The biggest consumption in the non-renewable resources is expected to occur in coal reserves with an annual rate of 1.7% for the same period. In particular, the coal consumption will fast increase in United States, China and India whereas it will decrease in OECD (Organization for Economic Cooperation and Development) countries, Europe and Japan. The difference is because the population growth in European countries and Japan is slow and also, renewable energy sources, such as biofuels, natural gas and nuclear power, are mostly preferred instead of coal. Despite the total increase of coal demand, world recoverable coal reserves reduced slightly from 1,145 billion tons in 1991 to 1,083 billion tons in 2000 but then much faster to 929 billion tons in 2006 (IEO, 2009). At the current production and consumption levels, it is estimated that economically recoverable coal reserves in the world will last for almost 200 years (Eastmidlands, 2009).

Another non-renewable resource in the world is petroleum. Although it has been the main energy source for a long time, world oil demand has decreased recently due to the global economic recession that began in 2008. In spite of this current low demand on the oil, it is believed that world oil prices will reach the highest value in 2012 and remain at this high level up to 2030. Therefore, as an alternative, the petroleum consuming countries prefer natural gas since it is less expensive. Additional benefit of using natural gas is that less carbon dioxide is emitted during usage of the natural gas than consuming coal or petroleum. As a result, total natural gas consumption is projected to increase by an average of 1.6% per year until 2030. To compensate the projected increase, the world's natural gas producers will need to increase supplies by 48 trillion cubic feet between 2006 and 2030 (IEO, 2009). Unfortunately, at this rate of

consumption, natural gas reserves left worldwide would last ~65 years (Eastmidlands, 2009).

Beside the diminishing of reserves and the rising prices for fossil fuels, the use of them releases carbon dioxide, the main cause of global warming, and also sulfur oxides and nitrogen oxides. On the other hand, the renewable energy is environmentally friendly energy type. Governments have initiated renewable research and development programs to increase the share of the use of renewable energy sources, such as solar, wind, biomass, geothermal and hydro. Hence, renewable energy sources are the fastest growing energy supply sources with 3% increase a year. Among many renewable energy sources, investment on hydroelectric and wind power seems to grow fast because technologies available for other renewable sources are not cost competitive with technologies available for fossil fuels (IEO, 2009). Although wind and hydroelectric power are fast growing energy sectors, they have some trivial drawbacks, such as effects on aqua and bird life, local flora and production of visual and noise pollution. These problems have been addressed and being resolved by many companies and universities supported by the government initiatives over the years. Nevertheless, renewable energy is currently more expensive than the fossil fuel energy (Iea, 2009).

Renewable energy seems to be promising but due to the technological problems and unsteady supply nature of renewable energy resources, they cannot fully replace the current fossil fuel economy in the long run. However, hydrogen economy is more likely to replace it since hydrogen is easily produced from variety of sources including renewable and also non-renewable energy sources. For instance, fuel cells are a clean technology with low emission levels and high energy efficiencies. Research and development spending on fuel cells worldwide is projected to rise from 10% in 2008 to 34% in 2018. High cost of fossil fuels, environmental concerns and low energy efficiencies of fossil fuel energy conversion technologies favor fuel cell commercialization; hence, expected sales growth over the coming decade in the industrialized countries. Also, the fuel cell sales will substantially increase in China and other developing countries, but the US, Western European countries, Japan, Canada and South Korea will account for more than four-fifths of all fuel cell demand in 2018 (World Fuel Cells, 2009).

The largest market for fuel cells is stationary electronic devices, such as electric power generators. It is expected to rise more than 40% annually and supply half of commercial demand in 2012 with different types of fuel cells, such as molten carbonate

fuel cells (MCFCs) and solid-oxide fuel cells (SOFCs). In addition, the market of portable electronic devices is expected to increase through 2012 since portable fuel cells, such as direct methanol fuel cells (DMFCs), seem to be viable candidates for replacing the most types of batteries due to better energy efficiencies, longer operational times and elimination of the need for recharging (Fuel Cells, 2008).

Turkey is the twenty third country based on the total energy consumption in the world (International Energy Data and Analysis for Turkey, 2009). Turkish government predicts that both petroleum and natural gas production will decrease in Turkey due to limited resources and fast economic growth but coal production – principally lignite – and renewable energy production will eventually increase to compensate the decrease in the reserves of petroleum and natural gas (Energy Policies of IEA Countries, Turkey, 2005). In fact, it is expected that coal demand would increase by 56% in 2010 and continue to increase till 2020 as a result of high lignite usage in power plants (Energy Policies of IEA Countries, Turkey, 2005). Unfortunately, in the long run, this demand cannot be supplied with domestic lignite production because of limited coal reserves. Unlike increased lignite production, General Management of Turkish Hard-coal Enterprises reported that the domestic production of hard coal declined between 1994 and 2007 (Report of Hard Coal Sector, 2009).

Turkish government has projected that oil demand in Turkey will have increased approximately 29 percent by 2020 although the oil consumption showed some decrease during the years of 2002 and 2003. Also, natural gas usage has increased in the world because of the global warming and lower market price. Unfortunately, both oil and natural gas reserves are limited in Turkey and their production cannot supply domestic consumption. According to the International Energy Agency, the oil reserves available in Turkey will last approximately another 18 years at current production rates. Moreover, although some new discoveries have recently been made in natural gas, natural gas will continue to be imported to supply the growing consumption in Turkey (Energy Policies of IEA Countries, Turkey, 2005). World Energy Council Turkish National Committee reported that 90 percent of 31 million tone of oil and approximately 30 billion cubic meter of natural gas was consumed in 2006 and all these fuels were imported (Energy Report of Turkey, 2005, 2006).

Alternatively, Turkey has substantial renewable energy resources. In fact, renewable makes the second-largest contribution to domestic energy production after coal. Among renewable energy sources, hydro and geothermal are the most used

renewable resources in Turkey. In addition, biomass is generally used in residential heating. Recently, investment on wind and solar energy power generators have been soaring because of Turkish government initiatives on wind and solar energy (Energy Policies of IEA Countries, Turkey, 2005). Moreover, fuel cell technology has been considered as future energy conversion systems and several industrial and academic projects have been implemented in Turkey in order to produce and develop some components of the fuel cells by private and government research centers, such as Ford-Otosan, Arçelik, Tofaş, TTGV, TUBİTAK (MAM) (Mam, 2009; Mmoistanbul, 2009). Why fuel is considered as alternative energy conversion system is because the fuel cell electrochemically converts the potential energy of a fuel to electricity in a highly efficient and environmentally acceptable manner. In a fuel cell, two chemicals – an oxidant and a fuel – react with each other so that the chemical potential was converted to the electricity. The operation principles of the fuel cells are similar to batteries; except that fuel cells do not need to be recharged and do not discharge like batteries. In addition to this, the fuel is not stored inside the fuel cell unlike batteries. This is advantageous for fuel cells because the amount of needed fuel can be changed disregarding the design of the cell and also the system can be recharged during operation (Iupap, 2009). Fuel cells have no moving parts so they are inherently reliable systems. In addition to this, fuel cells are low in maintenance, although, material degradation can occur due to the presence of reactants, various materials such as catalyst and various operating conditions including temperature and pressure ranges, but these are not costly maintenance (Shah, 2007; Shanna, 2004). Fuel cells are quiet and virtually pollution-free. The fuel cell power plant produces very little noise compared to conventional steam or gas turbine power plant. Noise is generated only from the fan or compressor used for pumping or pressurizing the cathode air. No ash or large volume wastes are produced from fuel cell operation (Shah, 2007). Moreover, CO_2, NO_x or SO_x emissions from the fuel cells are very low. If hydrogen is used as fuel, there are no emissions. In addition to all these advantages, fuel cells can be also used with various fuels such as hydrogen, methane, methanol, ethanol and biogas.

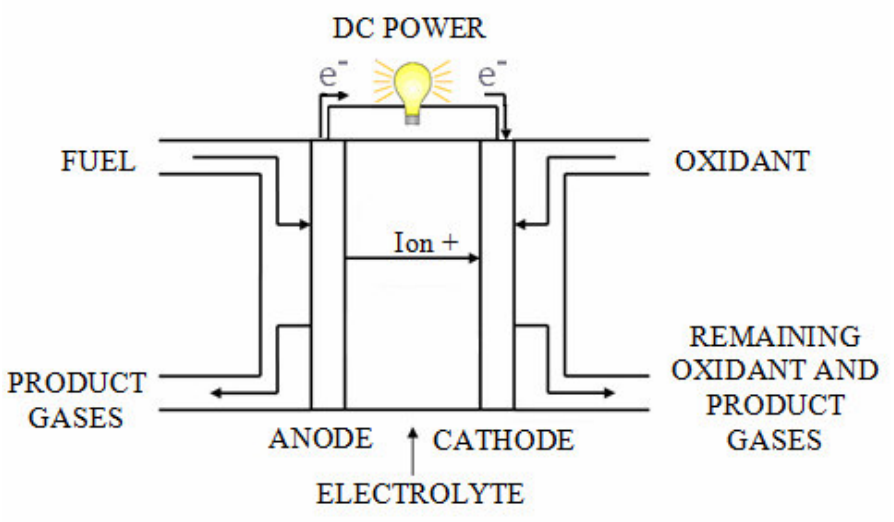

Figure 1.1. Simplified schematic of a fuel cell

Fuel cells consist of anode, anodic catalyst layer, electrolyte, cathodic catalyst layer, cathode, bipolar plates (interconnects) and gaskets for sealing or preventing leakage of gases between anode and cathode. The anode and cathode generally made of porous graphite thin layers which are responsible for gas diffusion and electron conductivity. Different kind of catalysts can be used depending on the fuel cell type but the most common catalysts for low temperature fuel cells and high temperature fuel cells are platinum and nickel, respectively. The electrolyte, that allows the ion transportation but isolates electrons, placed between two electrodes. Fuel cells may be connected electrically in both series and parallel known as stacks in order to provide large voltage and power output ranging from a few tens of watts to hundreds of watts.

The simplest expression of the fuel cell operation is that fuel is sent to the anode side and oxidant enters the cell through the cathode side. Electrons are released to the cathode side by external circuit and so electrical work is produced. At that time, ions flow across the electrolyte and the circuit is completed (Shah, 2007; Iupap 2009). The schema of the fuel cell was given in Figure 1.1.

Fuel cell can be classified with respect to following criteria; temperature, fuel type, oxidizer type or charge carrier (from the anode to the cathode or vice versa). However, the most common classification is by electrolyte type. The major types of fuel cells are: Proton Exchange Membrane Fuel Cells (PEMFC), Direct Methanol Fuel Cells (DMFC), Alkaline Fuel Cells (AFC), Phosphoric Acid Fuel Cells (PAFC), Molten Carbonate Fuel Cells (MCFC) and Solid Oxide Fuel Cells (SOFC). Table 1.1 shows

some features, such as application area and operating condition, of different fuel type cells.

Table 1.1. Types of fuel cells and their features
(Source: Shah, 2007)

	PEMFC	DMFC	AFC	PAFC	MCFC	SOFC
Primary applications	Automotive and stationary power	Portable power	Space vehicles and drinking water	Stationary power	Stationary power	Vehicle auxiliary power
Electrolyte	Polymer (plastic) membrane	Polymer (plastic) membrane	Concentrated (30-50%) KOH in H_2O	Concentrated 100% phospohoric acid	Molten Carbonate retained in a ceramic matrix of $LiAlO_2$	Yttrium-stabilized Zirkondioxide
Operating temperature	~100°C	~60 °C	~200 °C	~220 °C	~700 °C	~1000 °C
Charge carrier	H^+	H^+	OH^-	H^+	CO_3^{-2}	O^{-2}
Prime cell components	Carbon-based	Carbon-based	Carbon-based	Graphite-based	Stainless steel	Ceramic
Catalyst	Platinum	Pt-Pt/Ru	Platinum	Platinum	Nickel	Perovskites
Primary fuel	H_2	Methanol	H_2	H_2	H_2, CO	H_2, CO, CH_4
Start-up time	Sec-min	Sec-min		Hours	Hours	Hours
Power density (kW/m^3)	3.8-6.5	~0.6	~1	0.8-1.9	1.5-2.6	0.1-1.5
Combined cycle fuel cell efficiency	50-60%	30-40 % (no combined cycle)	50-60%	55%	55-65%	55-65%

Among all the fuel cell types, DMFC and PEMFC have similar structures, such as a polymer membrane as the electrolyte. The main difference is the fuel; methanol used in DMFC whereas H_2 used in PEMFC. Hydrogen must be either produced through reforming of suitable fuels or directly stored in a tank in order for PEMFC to operate. DMFC eliminates the needs of fuel reforming and also hydrogen storage. The elimination of these brings some benefits; for example; system simplicity, size, weight, dynamic behavior and cost. Since methanol is the fuel for DMFC, there are several advantages over the other fuels; such as the high energy density of methanol, quick start-up and refill, no problem of membrane humidification since methanol is fed with water at the start-up. In addition to these, methanol is a readily available as fuel so it is less expensive. Using liquid fuel rather than gas is another advantage of DMFC since it

is easier for transportation, storage and handle of methanol. In addition, since DMFC operates at approximately 60 ^{o}C, it is suitable for micro to mesoscale size applications where low power but higher energy density is required and also for the applications where lithium-ion batteries are used for portable power applications e.g. power cellular phones, laptops, camcorder. For portable applications, a DMFC (even with 3% system efficiency) would compete with the lithium-ion battery because methanol has an extremely high energy density (19.8 MJ/kg) than the lithium-ion batteries having an energy density of 0.6 MJ/kg (Fuel cells, 2009; Kakaç, 2008; Basu, 2007; Peter, 2001; Fernandez-Pello, 2002).

Beside the advantages of DMFC, the major drawback is the operation temperature. The electrical performance of DMFC decreases sharply below 60 ^{o}C by 5 times (Nakagawa et al., 2003). Also, it cannot be operated at temperatures below 50 ^{o}C so an external heater is needed for the room temperature start-ups and also low temperature operations. This temperature dependence operation of DMFC could be solved by using an external catalytic methanol combustion heater. Since methanol is already available, the combustion would be performed in a microreactor coupled with the DMFC; hence, eliminating external electrical heating to reach operating temperature.

The objective of this thesis is to investigate the effects of metal loading and the space velocity on the steady state temperature of the catalyst and on the time to reach at the temperature of 60 ^{o}C of a typical DMFC operating temperature in the methanol combustion occurring on an oxide supported metal catalyst started at room temperature and sub-room temperatures. For this purpose, alumina supported platinum catalysts (Pt/Al_2O_3) with varying Pt loadings were prepared using impregnation method and sol-gel made alumina.

The thesis contains five chapters. In chapter 1, energy consumption and demand in the world and Turkey with respect to the fuel types are introduced and general information about the new energy sources, the fuel cells, especially about DMFC is given. A literature survey on the methanol combustion on various catalysts, such as noble metal catalysts and metal oxide supported catalysts, is presented in details in Chapter 2. The subsequent Chapter 3 describes the specifications of the chemicals, the preparation and characterization of Pt/Al_2O_3 catalysts used in this thesis. Moreover, the experimental set-up of catalytic combustion of methanol and reaction conditions are explained in this chapter. Chapter 4 presents the performance of the catalysts as a

function of Pt loading and start-up temperatures for varying residence times. Finally, the thesis gives some conclusions and recommendations in Chapter 5.

CHAPTER 2

LITERATURE SURVEY

2.1. Methanol Combustion

Volatile organic compounds (VOCs) can be oxidized by two oxidation methods; thermal and catalytic oxidations. While thermal oxidation requires high temperatures, typically above 1000 ^{o}C, the catalytic oxidation operates at much lower temperatures. Also, it is important for the methanol volume percentage in air to be in the flammability limit (LFL: 6 %, UFL: 36 %) in order to have self sustained gas phase combustion. Otherwise, addition of another fuel or air must be supplied to ensure the combustion of methanol. On the other hand, the low temperature operation of catalytic combustion avoids the formation of toxic gases, such as NO_x, and particulates. Also, the catalytic oxidation can be carried out at methanol concentrations below the lower flammability limit. Therefore, the catalytic combustion of VOCs is more environmentally friendly than thermal oxidation.

Several studies have been focused on finding the best catalyst formulation for VOC oxidation and also the improvement of the activity of the catalyst. Among many possible catalyst formulations, the hydrophobic catalysts have been found to be highly active for VOCs destruction at relatively low temperatures and be less sensitive to deactivation through surface concentration of water (Sharma et al., 1995). Noble metal catalysts (such as Pt, Pd, Rh, Au) and metal oxides (Mn_2O_3, NiO, Cr_2O_3, V_2O_5) dispersed on high surface area support materials, such as alumina (Al_2O_3), silica (SiO_2) and titania (TiO_2), have been tested for the catalytic combustion of VOCs too. It was observed that the noble metal catalysts are generally used for non-halogenated VOC combustion while the metal oxide catalysts are for halogenated VOCs (Spivey, 1987). Methanol is one of the non-halogenated VOC and its combustion on a catalyst depends upon the type and nature of the catalyst. In fact, methanol oxidation is structure sensitive reaction.

The possible reactions of methanol in the absence and the presence of oxygen are given below with the heat of reactions and the Gibbs free energies at 298 K.

- Complete combustion of methanol;

$$CH_3OH + \tfrac{3}{2}O_2 \rightarrow CO_2 + 2H_2O \quad (2.1)$$

$$\Delta H_{rxn} = -674kJ/mol, \Delta G_{rxn} = -690kJ/mol$$

- Incomplete combustion of methanol;

$$CH_3OH + O_2 \rightarrow CO + 2H_2O \quad (2.2)$$

$$\Delta H_{rxn} = -393kJ/mol, \Delta G_{rxn} = -432kJ/mol$$

- Partial oxidation of methanol;

$$CH_3OH + \tfrac{1}{2}O_2 \rightarrow CO_2 + 2H_2 \quad (2.3)$$

$$\Delta H_{rxn} = -193kJ/mol, \Delta G_{rxn} = -232kJ/mol$$

- Oxidative dehydrogenation of methanol;

$$CH_3OH + \tfrac{1}{2}O_2 \rightarrow CH_2O + H_2O \quad (2.4)$$

$$\Delta H_{rxn} = -157kJ/mol, \Delta G_{rxn} = -176kJ/mol$$

- Dehydration of methanol;

$$2CH_3OH \leftrightarrow CH_3OCH_3 + H_2O \quad (2.5)$$

$$\Delta H_{rxn} = -24kJ/mol, \Delta G_{rxn} = -16kJ/mol$$

- Dehydrogenation of methanol;

$$CH_3OH \leftrightarrow CH_2O + H_2 \tag{2.6}$$

$$\Delta H_{rxn} = +84kJ/mol, \Delta G_{rxn} = +53.1kJ/mol$$

- Decomposition of methanol;

$$CH_3OH \rightarrow CO + 2H_2 \tag{2.7}$$

$$\Delta H_{rxn} = +90kJ/mol, \Delta G_{rxn} = +26kJ/mol$$

It can be said that the most favorable reaction among all these methanol reactions is the complete combustion of methanol since it has the lowest Gibbs free energy.

2.2. Catalysts for Methanol Combustion

2.2.1. Noble Metal Catalysts

The activity of the combustion reactions at low temperatures and selectivity to the carbon dioxide and water formation is very high on noble metal catalysts (Spivey et al., 2004). For instance, McCabe et al. studied on various noble metal catalysts such as rhodium (Rh), silver (Ag), cupper (Cu), platinum (Pt) and palladium (Pd) in order to test the activity of methanol oxidation. Among these catalysts, platinum and palladium were found to have higher activity for methanol oxidation than the others (McCabe et al., 1986). In addition to McCabe research group, metals other than platinum and palladium were found to have lower activity for combustion because they undergo sintering, volatility losses (loss of metal components through volatilization) and irreversible oxidation at high temperatures (Prasad et al., 1984; Spivey et al., 2004).

In addition to these noble catalysts, gold (Au) has been also studied in recent years as a catalyst for methanol oxidation reactions. It was found that the selectivity and

conversion on Au catalyst was low as compared with Pt. Furthermore, stability of Au at high temperatures was the major problem (Bond et al., 1999; Xu et al., 2008).

In other studies, Pt catalysts were found to be more active as compared with Pd catalysts for the methanol oxidation. The low activity of the palladium catalysts was claimed to be due to the weak adsorption of oxygen on Pd crystallites (Gates et al., 1979; Sharma et al., 1995). Pt catalyst has higher activity for oxidation reaction and good stability; hence it is also commonly used as the best monometallic catalyst in the electrooxidation of methanol (Ferrin et al., 2009).

2.2.2. Metal Oxide Supported Catalysts

Supports are generally used to improve the dispersion of the catalytically active phase which usually consists of nano sized metals or oxides.

Group VIII and IB transition metals, such as Pt, Ir, Pd, Rh, Ru, Ni, Co, and Au, Ag, Cu, can easily form in nano sized metal/metal oxide. The heat of formations of the oxides of these metals are low (usually below $-\Delta H_f$ = 40 kcal/mol). Therefore, the oxides of these metals can easily be reduced using a reducing agent, such as hydrogen. However, a complete reduction of metal oxides with high heat of formation, above 100 kcal/mol, such as SiO_2, TiO_2, ZrO_2, $A1_2O_3$, CeO_2, Nb_2O_5, MgO and La_2O_3 is difficult so they are generally used as catalyst supports (Spivey et al., 2004).

The effect of supports on stability of the nanosized metal catalyst in methanol oxidation has been investigated by several research groups. It was found that the stability of metal catalyst and its oxides were observed to be dependent on the choice of support (Croy et al., 2007).

Minicò and coworkers studied the catalytic oxidation of methanol on coprecipitated Au/Fe_2O_3 catalysts in the presence of excess of oxygen. They found that the higher catalytic activity achieved and light-off temperature decreased by increasing the gold content in the catalyst. While the oxidation reaction of methanol started at 80 ^oC and reached the total conversion at 160 ^oC with 8 wt% gold catalyst. However, the oxidation started at 180 ^oC and reached the total conversion at temperatures higher than 270 ^oC over undoped Fe_2O_3 catalyst. It was claimed that the gold particles weakened the strength of the Fe–O bonds; hence, increasing the mobility of the lattice oxygen which is involved in the oxidation reaction. In addition to achievement of high activity and low

light-off temperature over Au/Fe_2O_3 catalyst, none of the intermediate oxidation compounds were detected during the methanol oxidation. CO_2 was formed as the only product by direct oxidation because formaldehyde (one of the intermediate oxidation products) was very reactive on Au/Fe_2O_3 to form CO_2 easily (Minicò et al, 2000).

Furthermore, Pt particles were deposited on reducible (CeO_2, TiO_2) and non-reducible (SiO_2, ZrO_2, Al_2O_3) supports to test in the methanol oxidation. It was found that direct decomposition of methanol occurred on all the supported catalysts. Pt on ZrO_2 support was found the most active catalyst for methanol oxidation and claimed that the Lewis acid sites on the surface affected the electronic state of the supported particles, Pt. Moreover, it was pointed out that oxidation state of Pt was more important parameter than the reducibility of the support (Croy et al., 2007).

The reduced form of the reducible supports is often labile and can diffuse onto the metal which affects the catalytic activity. This is called strong metal support interaction (SMSI).

Alumina supported platinum (Pt/Al_2O_3) catalyst was also studied by Hinz and coworkers. They tested the effect of three different Pt loadings (0.1, 1.0 and 3.0 wt %) on the catalytic performance, high activity and stability. The best performance at low temperature -i.e. maximum CO_2 conversion- achieved at a temperature range of approximately 90- 125 ^oC – was obtained with 3.0 wt% Pt/Al_2O_3 catalyst (Hinz et al., 2002).

Al_2O_3 support and Li_2O and CeO_x doped Al_2O_3 were used and tested not only with Pt but also with Cu, Ag and Au metal catalysts. Although Au/Al_2O_3 was found to be the most active catalyst -i.e. methanol oxidation started at 100 ^oC- and the maximum conversion reached 100% at 275 ^oC and also, Cu/Al_2O_3 was the most active in the complete oxidation and showed the highest selectivity to CO_2. Moreover, addition of CeO_x increased CO_2 selectivity (Lippits et al., 2009).

In addition to the supported monometallic catalysts, the activity of bimetallic catalysts was also investigated. Chantaravitoon and coworkers compared the monometallic Pt/Al_2O_3 with alumina supported on bimetallic, Pt–Sn, catalyst. The alumina-supported monometallic Pt catalyst was found to be the most active catalyst for methanol oxidation (Chantaravitoon et al., 2004). In addition to Sn metal, $Pt/\gamma\text{-}Al_2O_3$ catalysts doped with magnesium (Mg) were also examined for methanol oxidation. The main purpose of using Mg was to improve the activity of the catalysts for the low-temperature operations. However, it was observed that addition of Mg decreased the

low-temperature activity for methanol oxidation (increasing Mg loading from 0.6% to 4.7% increased the light off temperature approximately 35 ^{o}C). Another study reports that Al_2O_3 is more reactive than MgO for methanol oxidation (Badlani et al., 2001). Therefore, by considering these two results, it was claimed that Mg species blocked the Al_2O_3 surface and the platinum dispersion was considerably decreased with a high Mg loading so that the activity of the catalyst decreased with adding Mg (Arnby et al., 2004). In addition, Álvarez-Galván and coworkers also studied bimetallic activity and reported that the low-temperature activity could be achieved on Pd-Mn/Al_2O_3 (complete combustion was achieved at ambient temperature on 1% Pd, 18.2% Mn). The higher activity of the bimetallic Pd-Mn catalyst than the monometallic Pd was explained that not only the PdO_x moiety but also the PdO_x–MnO_x participate in the oxidation reaction (Álvarez-Galván et al., 2004).

Considering all the studies about supported metal catalysts, it could be concluded that the supports participate in the catalytic reactions and Lewis acidity plays a crucial role in modifying the reactions at the interface since the morphology of the adsorbed reactants are dependent on the electronic state of the supported metals. In addition to this, the interaction between the metal and the alkali contained in the support may also influence both the physical properties of the metal and its activity.

2.3. Reaction Mechanism of Methanol Oxidation on Different Catalysts

Studies on the reaction mechanism of methanol oxidation on a catalyst exhibit that the mechanism of catalytic oxidation depends upon the type of catalyst. In other words, the structure of the catalyst affects the reaction mechanism. For instance, while methanol oxidizes directly to CO_2 without forming CO on Pt(111) crystalline plane, methanol oxidizes to CO first, then CO_2 on the Pt(100) crystalline plane. Moreover, the more open (100) surface binds all the intermediates more strongly than the closer-packed (111) surface so that CO poisoning will be much stronger on the Pt(100). This could be explained by the highest reactivity of Pt(100) surface because (100) crystalline plane has a closer d-band center to the Fermi level compared to the (111) facet (Ferrin et al, 2009).

Gold and platinum catalysts for methanol oxidation were also investigated. It was found that the difference between using Au and Pt catalyst as an oxidation reaction is the reaction pathway. If gold was used as a catalyst, methanal (CH_2O) is formed as the primary product of the reaction. Methanal then oxidized directly to carbon dioxide. However, on platinum, carbon monoxide is formed before the carbon dioxide (Bond et al., 1999; Xu et al., 2008).

In another study, gold was supported by titania to investigate the behavior of the reaction mechanism of methanol oxidation. At the end of the reaction, on Au/TiO_2 catalyst, the product stream was found to contain CH_4, CO, CO_2, H_2O and H_2 (Nuhu et al., 2007).

Mechanisms of methanol oxidation were also investigated on Al_2O_3 supported Cu, Ag and Au catalysts by Lippits et al. All the three Al_2O_3 supported metal catalysts showed the same mechanism which consisted of two-steps. In the first step, methanol was dehydrogenated on alumina to form formaldehyde (methanal) with a high selectivity; then in the second step, the formaldehyde oxidized on the metal particles to CO or CO_2 (Lippits et al., 2009).

The same reaction steps proposed by Lippits et al. was also observed by Cao et al (Cao et al., 2009). Therefore, it can be said that both metallic sites and Lewis acid sites are required for activating oxygen and substrate molecules, respectively (Spivey et al., 2004).

Cao et al. (Cao et al., 2009) studied the methanol decomposition on Al_2O_3 and Pt/Al_2O_3 catalysts. Dissociative adsorption of methanol was observed on both catalysts. A surface hydroxyl group was also produced as a result of the dissociative adsorption and it desorbed by forming H_2O.

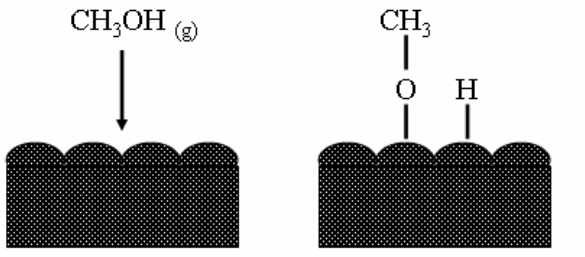

Figure 2.1. Dissociation adsorption of methanol on a surface

However, one of the differences between methanol adsorption on Al_2O_3 and Pt/Al_2O_3 was reported that the formation of CO and H_2 on Pt/Al_2O_3 was observed as compared to that on Al_2O_3 at the beginning of the adsorption which showed that Pt played a key role in the formation of CO and H_2. The other difference was in the CO_2 formation. CO_2 was produced only by formate ($COOH^-$) decomposition on the Al_2O_3 support. However, two reaction pathways were claimed that to be possible for CO_2 formation on Pt/Al_2O_3 catalyst: CO_2 could be formed from formate decomposition to CO followed by CO oxidation or could result directly from formate decomposition in the absence of O_2 by heating (Cao et al., 2009).

2.4. Particle Size Effect on Catalytic Performance

For metal catalyzed reactions, the metal particle size plays a crucial role on the catalytic performance for the structure sensitive reactions. Thus, light-off temperature of methanol combustion could be reduced from high temperatures by changing the particle size of the catalyst.

Nano-size particles are significantly more reactive than their bulk counterparts and can be used to enhance the performance of catalytic combustors. For instance; the Pt particles with 2-5 nm and 200 nm are more reactive than 500 nm particles for methanol combustion. Furthermore, the high surface area of the particles and associated number of active sites enhance the reactivity (Ma et al., 2008).

Particle size effect on catalytic performance has been also reported by Croy and coworkers for large (~15–18 nm) and small (~8–9 nm) Pt particles deposited on ZrO_2 support in the methanol oxidation. They found that the catalyst with small Pt particles was more active than the catalysts with large particles (Croy et al., 2007).

2.5. Microreactor Systems

The term ‘microreactor’ means a small tubular reactor for testing catalyst performance. The smaller size and multiple functions of microreactors make them suitable for low cost operation and easier mass production than conventional macroscopic reactor systems. However, the challenge in the microreactor is the excessive pressure drop. However, pressure drop problem could be reduced by splitting

the flow into multiple channels while maintaining the reactor throughput and the high surface to volume ratio at the same level (Jensen et al., 2001).

Micro-channel bed reactors have more advantages than packed bed reactors, such as the enhanced heat and mass transfer, a high surface to volume ratio, the flow uniformity, a low pressure drop and a safe control in explosive regime (Leu et al., 2010; Ryi et al., 2005). Beside of these advantages of micro-channel bed reactors, they have some disadvantages. For instance; the small channels can be blocked due to the effect of carbon formation for combustion reactions. Moreover, the catalysts buried in the microchannels cannot easily be replaced after the deactivation (Avcı et al., 2010).

Various reactions, such as hydrogen combustion, on microcatalytic combustors with Pt/Al_2O_3 coated materials were studied for a heat source of methanol steam reformer (Jin et al., 2010) and micro-gas sensor application (Nishibori et al, 2008).

In addition to Jin and coworkers, Leu et al. used microcatalytic combustors as a heat source of methanol steam reformer, but they performed methanol combustion instead of hydrogen combustion. They compared the efficiency of a packed bed and a micro-channel bed reactor in the methanol catalytic combustion. They used the same weight Pt/Al_2O_3 catalyst at the same space velocity for the two different reactors and found that the concentration of CO_2 formation in the micro-channel bed was over 2 times that in the packed bed. In addition to this, they studied with the same contact area catalyst and obtained that although the weight of the catalyst in the packed bed reactor was 4.9 times higher than in the micro-channel bed reactor, the concentration of CO_2 formation in the micro-channel bed was 39% higher than that of the packed bed (Leu et al., 2010).

In the literature, various metal and metal oxide and supported catalysts nave been tested for finding the best catalytic performance for different applications. However, it should be noted that the methanol combustion on Pt/Al_2O_3 catalyst was not studied below room temperature and was not used as a heat source for DMFC. Therefore, the thesis focused on investigating the start-up catalytic performance of the combustion reaction at room temperature and also below the room temperatures to find out a start-up time and also steady state the reaction temperature to supply the adequate level of heat for the DMFC operating at room temperature and sub-room temperature.

CHAPTER 3

MATERIALS AND METHOD

3.1. Materials and Equipment

Alumina (Al_2O_3) sol was prepared by a modified sol-gel method for coating and also obtaining powder. Briefly, aluminum isopropoxide (AIP, Alfa Aesar) and nitric acid (HNO_3) were used as a precursor and peptizing agent, respectively. Moreover, glycerol and polyvinyl alcohol (PVA) (in 1 and 2 wt.%) were used in Al_2O_3 preparation to increase the porosity of the catalyst. In addition to pure Al_2O_3, alumina supported platinum (Pt/Al_2O_3) powder catalysts having the Pt loadings of 1-5 wt.% were prepared by impregnation method. The properties of the materials used in the catalyst preparation are given in Table 3.1.

Table 3.1. Properties of materials used in catalyst preparation.

Chemicals	Chemical formula	Molecular Weight (g/mol)	Purity (%)
Aluminum isopropoxide	$Al[OCH(CH_3)_2]_3$	204.24	98
Platinic acid	$H_2PtCl_6.6H_2O$	517.91	99.9
Glycerol	$C_3H_5(OH)_3$	92.09	98
Polyvinyl alcohol	$[-CH_2CH(OH)-]_x$-$[-CH_2CH(O_2CCH_3)-]_y$	9000-10000	98

Dip coating machine (NIMA Technology) was used for the coating alumina on stainless and aluminum plates. Before the coating, the viscosities of the alumina sols were measured by Canon Fenske tube or Brookfield Rheometre (RV DV-III).

3.2. Methods

In this study, the experiments can be categorized into three groups: catalyst preparation, catalyst characterization and catalytic combustion of methanol.

3.2.1. Catalyst Preparation

Alumina catalysts with different concentrations were coated on both stainless steel and aluminum plates and alumina supported platinum catalysts with different platinum loadings were prepared.

3.2.1.1. Preparation of Alumina Coated Plates

Alumina coated plates were prepared by the dip coating process. The first step of the preparation of Al_2O_3 support was the hydrolysis of AIP. In this step, AIP and water were mixed in the concentrations of 0.02, 0.04, 0.07, 0.09 and 0.12 g/ml at 85 ^oC and stirred for 1 hour. The second step is the peptization in which HNO_3 was added to the mixture at the same temperature and kept stirred for additional 1 hour. At the end of 1 hour, sol was obtained and waited until the temperature of the sol reached the room temperature for coating.

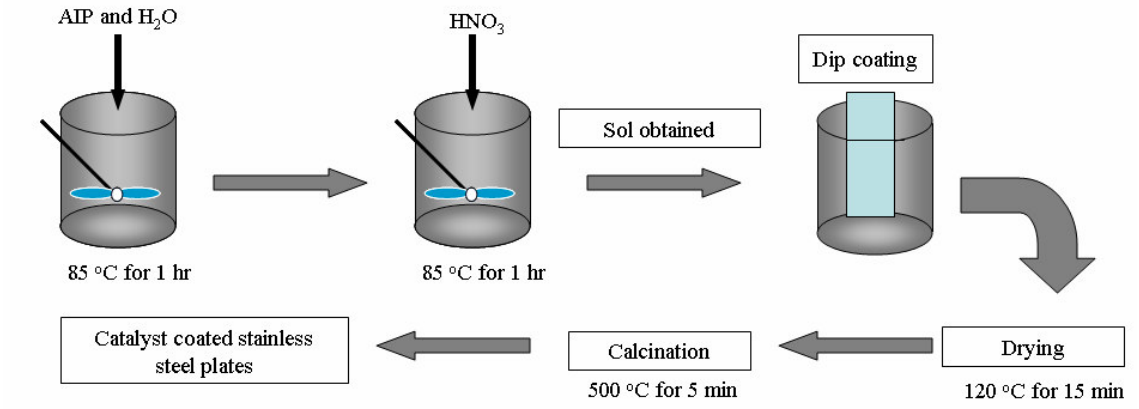

Figure 3.1. Catalyst coated plate preparation procedure without additive

If it was necessary to increase the porosity of the catalyst, an additive (such as glycerol or PVA) were added to AIP-water mixture at the same temperature and stirred

for 3 hours before the peptization step. Then, pre-cleaned stainless steel and aluminum plates were dipped into the sol for coating. Finally, the coated plates were dried at 120 ^{o}C for 15 minutes and then, calcined at 500 ^{o}C for 5 minutes for the sol without additives. When the sol had additives, the plates were dried at 120 ^{o}C for 30 minutes and calcined at 500 ^{o}C for 15 minutes. The catalyst coated plate preparation procedures without and with additives are given in Figure 3.1. and Figure 3.2., respectively.

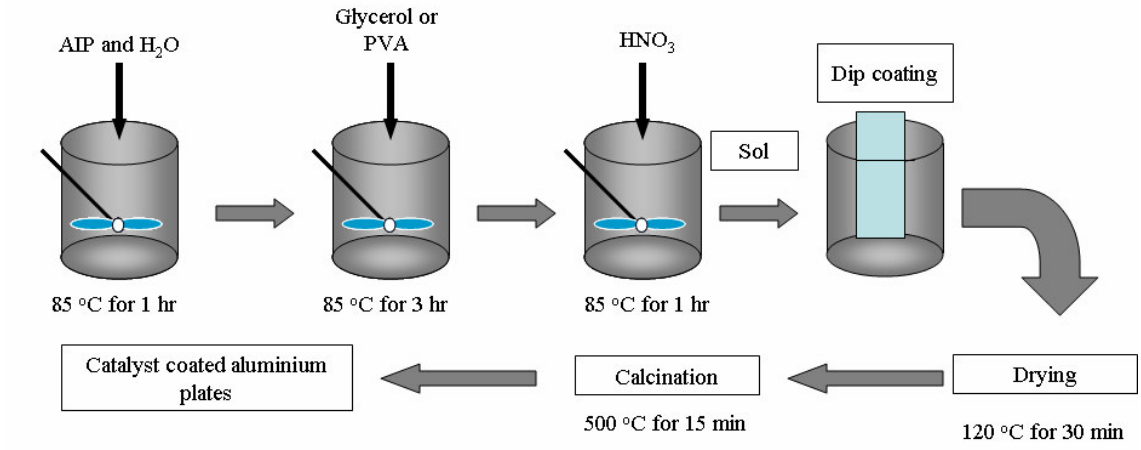

Figure 3.2. Catalyst coated plate preparation procedure with additive

3.2.1.2. Preparation of Alumina Supported Platinum Catalysts

Alumina supported platinum catalysts were synthesized in order to use in a micro-packed bed reactor. The same procedure in section 3.2.1.1. was applied for the preparation of the alumina support with glycerol but the catalyst was dried at 120 ^{o}C over night and then, calcined at 500 ^{o}C for 6 hours. Finally, incipient wetness impregnation method was used for loading platinum on the alumina support. The catalysts were sieved to 60 mesh (250 μm) before the impregnation.

The incipient wetness impregnation procedure was as following;

1. Pore volume of the alumina was found.
2. Platinum precursor was weighed for required Pt loading (1-5 wt % loading).
3. The platinum precursor containing solution was added slowly to the alumina support.
4. The catalyst was dried at 120 ^{o}C over night.
5. The catalyst was calcined at 300 ^{o}C and 500 ^{o}C for 6 h.

3.2.2. Catalyst Characterization

The catalysts were characterized by several techniques, such as N_2 adsorption, X-Ray Diffraction (XRD) and Scanning Electron Microscopy (SEM).

3.2.2.1. Textural Properties

The total surface areas, pore volumes, average pore diameters and pore distributions of the catalysts, were determined by N_2 adsorption at 77.34 K using ASAP2010. Before the analysis, the calcined samples were dried at 120 ºC over night.

3.2.2.2. X-ray Diffraction (XRD)

The crystalline structure and the average crystallite sizes were determined. The XRD spectra of the catalysts were measured by using a Philips Xpert XRA-480 Model X-ray diffractometer. The average crystallite sizes were calculated using Scherrer equation.

3.2.2.3. Scanning Electron Microscopy (SEM)

Philips XL30S model scanning electron microscope was used for the surface morphology analysis and the surface chemical compositions. All the samples were coated with gold prior the analyses to avoid the adverse effect of charging on the SEM images.

3.2.3. Catalytic Combustion of Methanol

Catalytic combustion of methanol was performed in a glass tube reactor filled with Pt/Al_2O_3 catalysts. The reactor set-up is shown in Figure 3.3.

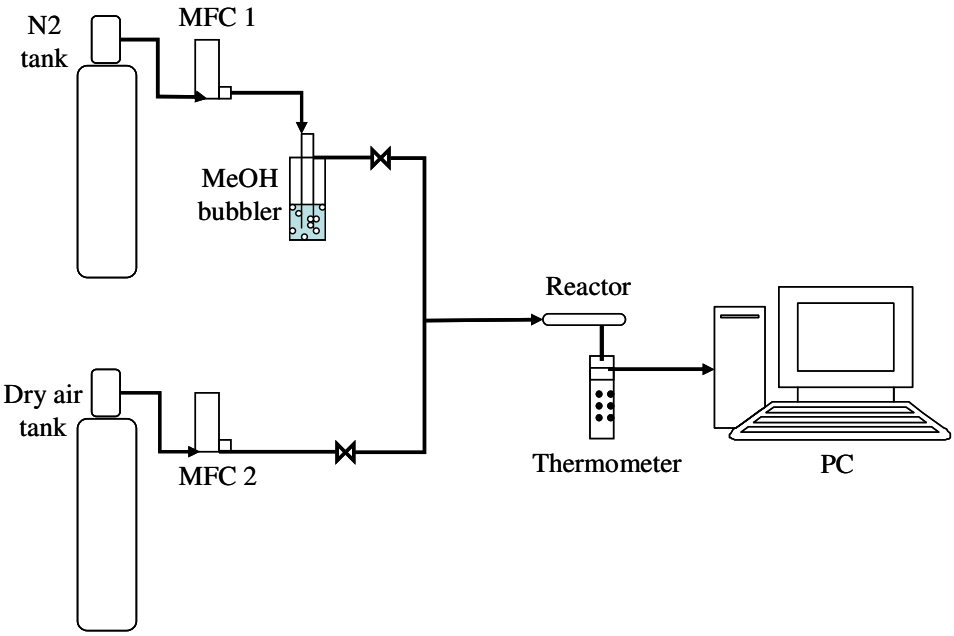

Figure 3.3. Experimental set-up of methanol combustion

Methanol at room temperature was put in a bubbler and nitrogen was sent through the bubbler in order to vaporize methanol. Dry air from the tank was mixed with nitrogen and methanol vapor and then, the gas mixture was sent to the reactor. The reactor was a glass tube with 5 mm ID., 8.2 mm OD., and 76.2 mm in length. The catalyst was supported between the two glass wool plugs.

The concentration of air and nitrogen were adjusted with mass flow controllers (Brooks model 5850) MFC1 and MFC2, respectively. Reaction temperature was measured on the reactor surface with a K-Type thermocouple and recorded continuously using online PC.

Pt/Al_2O_3 catalyst was activated before the activity tests. First of all, the catalyst was calcined at 400 ^oC for two hours in order to get rid of the adsorbed species, the reaction products. Then, at room temperature, it was washed with 1.5 ml of methanol for the activation and methanol was drained by dry air for few seconds. Finally, the

washed catalyst was dried at 120 ^{o}C for one hour and it was ready for the reaction. In addition to this activation procedure, the catalysts were also tested without activation procedure. In this case, when the reaction temperature was at steady state, the methanol and nitrogen mixture stream was closed and the reactor exposed to only dry air flow until the reactor temperature reached the initial temperature.

Reaction was performed within the temperatures range of from -15 ^{o}to +28 ^{o}C. Methanol composition was kept at 0.4 % and the total flow rate was changed from 22 to 50 ml/min.

CHAPTER 4

RESULTS AND DISCUSSION

4.1. Methanol Combustion

The catalytic activities of Pt loaded Al_2O_3 catalysts were tested in methanol combustion in a tubular reactor at room and sub-room temperatures. The reactor temperature was used as a measure of catalytic activity and indicated if methanol combustion occurred on these catalysts.

The activity of the catalysts was tested both with and without the activation procedure. These procedures were explained in detail in Chapter 3. In this study, the catalyst was defined as fresh catalyst when activation procedure was applied whereas without activation procedure, the catalyst was defined as the reused catalyst.

Before the beginning of the activity tests, internal and external mass transfer limitations were checked for a catalyst having particles sizes less than 250 μm. 250 μm particle size was chosen based on previous studies in order to eliminate internal mass transfer limitation and also avoid excessive pressure drop. External mass transfer limitation is known to be avoided by increasing the total flow rate; resulting in decreased film thickness around the catalyst particles. Therefore, only three different flow rates (22 ml/min, 35 ml/min and 50 ml/min) due to the limitations of the flow controllers were used at the same space velocity in order to check if there was the external mass transfer limitation at these flow rates. Steady state reaction temperature was determined at each flow rate. Figure 4.1 shows that the reaction temperature stayed nearly the same after 50 ml/min of the total flow rate. In fact, this is in parallel to the previous studies since 50 ml/min was reported to be enough to eliminate the external mass transfer limitation (Schiffimo et al., 1993). Thus, all the activity tests were performed at the total flow rate of 50 ml/min.

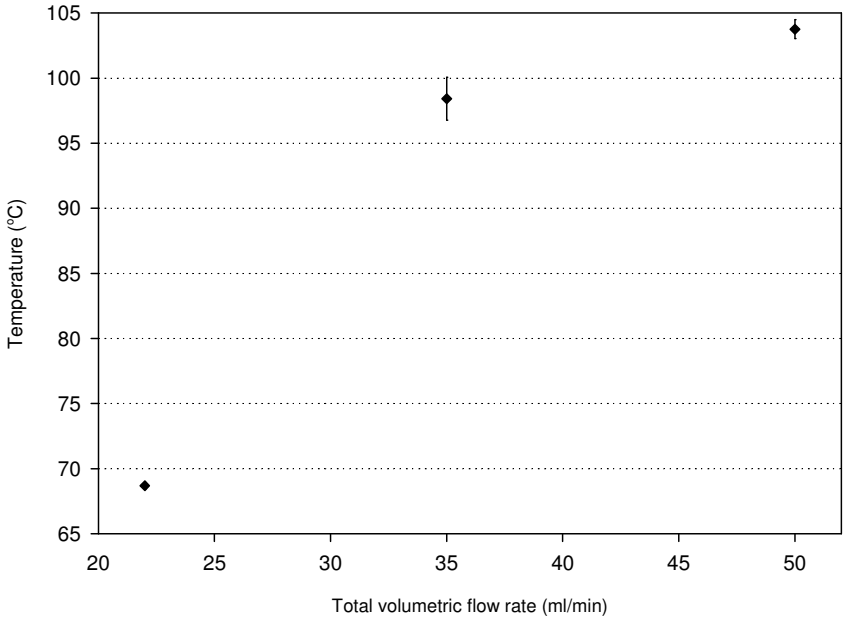

Figure 4.1. Tests for external mass transfer limitation (2% Pt/Al_2O_3, 0.4 % CH_3OH, T_{in}=28 ^oC, T_{amb}=23 ^oC, SV=2.4 s^{-1}, catalyst amounts: for V_T=22 ml/min, 0.1101 g; for V_T=35 ml/min, 0.2297 g; for V_T=50 ml/min, 0.3696g without activation procedure)

In order to make better comparisons between the catalysts used in this study, adiabatic flame temperature for the methanol combustion (0.4% methanol in air) was calculated. Table 4.1 indicates that the adiabatic flame temperature changes with the conversion for a inlet concentration of 0.4 wt.% methanol in air and the maximum adiabatic temperature of 117 ^oC would be achieved at 100% methanol conversion. The calculations are given in Appendix B.

Table 4.1. Adiabatic flame temperature with conversion (V_T=50 ml/min, 0.4% CH_3OH)

X_{CH3OH}	1	0.9	0.8	0.7	0.6	0.5	0.4	0.3	0.2	0.1
$T_{adiabatic}$ (^oC)	117	108	99	90	80	71	62	53	43	34

4.1.1. Effect of Pt Loading on Methanol Combustion

Figure 4.2 shows the reaction temperature profile for the methanol combustion on the undoped and varying Pt loaded Al_2O_3 catalysts. The initial temperature of the reactors was between 27 ^oC and 28 ^oC and the other operating conditions were given in the figure caption. As soon as the feed mixture was fed to the reactor initially at 27-28 ^oC, the temperature of the reactor increased with the time and reached at a maximum temperature which was the steady state temperature.

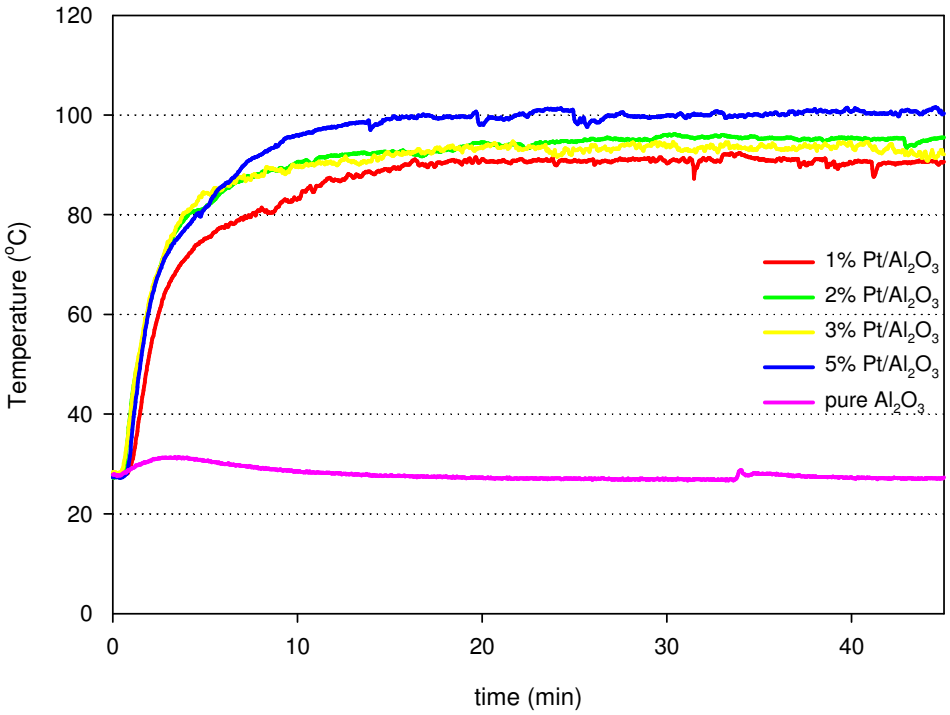

Figure 4.2. Effect of Pt loading on reaction temperature (0.4% CH_3OH, V_T=50 ml/min, T_{in}=27-28 ^oC T_{amb}=24-26 ^oC, SV=2.4 s^{-1}, catalyst amounts: for 5% Pt/Al_2O_3, 0.3771 g;, for 3% Pt/Al_2O_3,0.3985g; for 2% Pt/Al_2O_3, 0.3746 g;, for 1% Pt/Al_2O_3, 0.3713 g; and for Al_2O_3, 0.3721 g)

It was observed that there was a small increase in the temperature from 28 ^oC to 31 ^oC in 2 minutes on the undoped Al_2O_3 and then stayed constant for approximately 2 minutes before decreasing to the initial reactor temperature. It seems that this temperature increase did not result from the methanol combustion; it might be due to either the adsorption or dehydration of the methanol on the Al_2O_3 surface (Schiffimo et al., 1993). The dissociative adsorption and the dehydration energy of methanol on the Al_2O_3 surface is 65.81 kJ/mol and 111.89 kJ/mol, respectively (Lee et al., 2006). Hence,

the reactor temperature increased until all the Al_2O_3 surface was coated with the methanol molecules or the dehydration products. Then, it started to decrease to the initial temperature. This is plausible since the specific surface area of the pure alumina is ~316 m^2/g. On pure alumina, a small temperature spike with a magnitude of 1 ^oC, seems to be due to temperature reading and/or flow rate fluctuations inside the bubbler.

In contrast to pure alumina, Pt/Al_2O_3 catalysts with 1%, 2%, 3% and 5% Pt loadings were very active in methanol combustion starting at room temperature. The steady state reaction temperatures for 1%, 2%, 3% and 5% Pt/Al_2O_3 catalysts are 90, 95, 94 and 100 ^oC, respectively. 2% and 3% Pt/Al_2O_3 reach at the same steady state temperature and also it seems that 1, 2 and 3% Pt catalysts have almost the same steady state temperature within the experimental error whereas there is a significant difference in the steady state temperatures between 1% and 5% Pt catalysts. This may be explained due to the varying Pt size and its distribution on Al_2O_3.

One may speculate that if the Pt crystallites are assumed to be the same size with narrow size dispersion on Al_2O_3, it should be expected that the activity of the catalyst increases with Pt loading due to the increased active sites or the higher activity could be explained by the increased number of available active sites at the Pt-Al_2O_3 interface (Hinz et al., 2002). In fact, higher the combustion activity, higher the heat release; hence, resulting in higher temperature. This expectation seems to be consistent with increasing Pt loadings but it is not clearly observed between 1, 2 and 3% Pt loadings and between 2, 3% and 5% Pt loadings as compared to a significant difference observed between 1 and 5% Pt loadings.

In addition to steady state temperature of the catalysts, start-up time to reach at DMFC operation temperature from room temperature is also important factor in assessing the catalytic combustion performance of the catalysts. Therefore, all the catalysts are compared as a function of Pt loadings for the time necessary to reach at the temperature of 60 ^oC of a typical DMFC operating temperature as shown in Figure 4.3. 2%, 3% and 5% Pt/Al_2O_3 catalysts reached at 60 ^oC in ~ 114 seconds, but it took ~150 sec for 1% Pt/Al_2O_3 to reach at the same temperature. If one compares the steady state temperatures for all the catalyst, it seems that the average crystallite size of Pt and the crystallite size distribution on 2%, 3% and 5% Pt/Al_2O_3 would be similar so that the steady state temperatures are the same within the experimental error whereas 1% Pt/Al_2O_3 may have significantly different crystallite size and the distribution than that of

5%Pt/Al_2O_3. This is in parallel with the literature study since the methanol combustion reaction is structure sensitive (Ma et al., 2008).

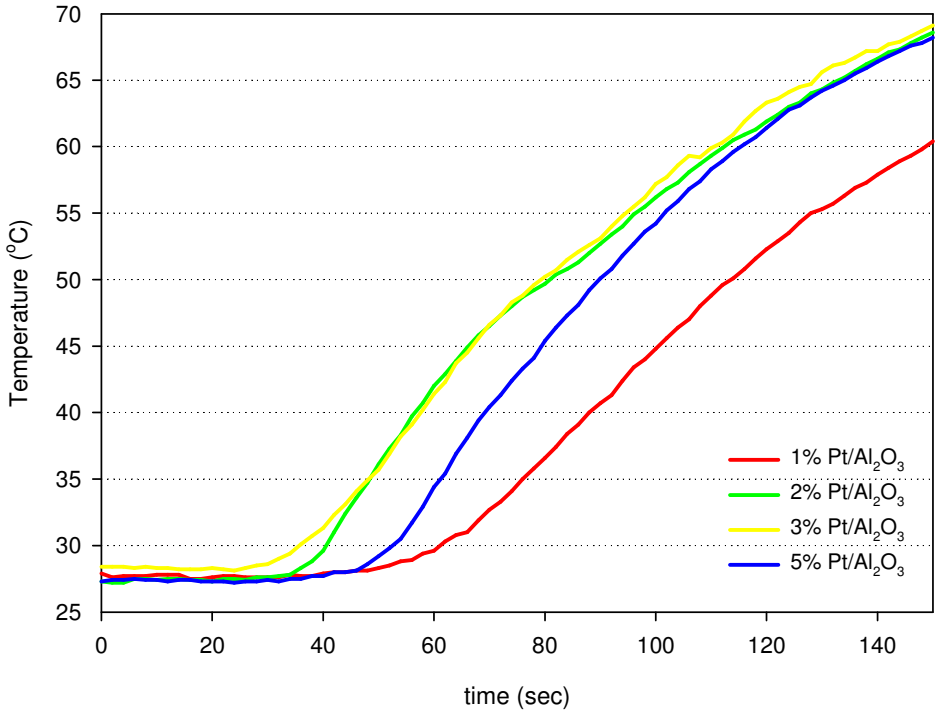

Figure 4.3. Effect of Pt loading on time to reach at DMFC operation temperature (0.4 % CH_3OH, V_T=50 ml/min, T_{in}=27-28 °C, T_{amb}=24-26 °C, SV=2.4 s^{-1})

By considering the steady state temperature and the time to reach the temperature of DMFC operation, although 5% Pt loading resulted in a higher steady state temperature than 2% Pt loading, both catalysts reached at 60 °C at the same time. Hence, 2% Pt loading seems to be optimal for methanol combustion under the operating conditions used in this thesis when considering the price of platinum.

4.1.2. Effect of Space Velocity on Methanol Combustion

The degree of surface coverage of reaction intermediates is important parameter on catalytic activity of the catalytic reactions. This could be controlled by changing reaction conditions, especially, space velocity (Lee et al., 2000). In this study, three different space velocities with 15% increment (2.4 s^{-1}, 2.8 s^{-1} and 3.1 s^{-1}) were tested on fresh and reused 2% Pt/Al_2O_3 catalyst to observe the effect of space velocity on the activity under the same reaction conditions used before. The temperature profiles of

these reactions are given in Figures A1-A3. and A7-A9 in Appendix A. The space velocity is defined as the ratio of total feed volumetric flow rate (measured at room temperature and 1 atm pressure) to the catalyst volume.

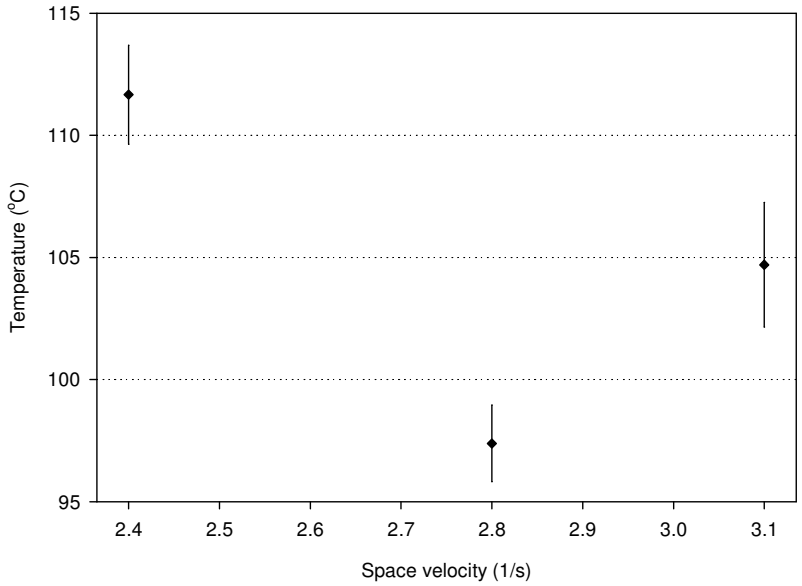

Figure 4.4. Effect of space velocity on steady state temperature for fresh catalyst (2% Pt/Al_2O_3, 0.4% CH_3OH, V_T=50 ml/min, T_{in}=28 ^oC, T_{amb}=23 ^oC, catalyst amounts: for SV=3.1 s^{-1}, 0.2624 g; for SV=2.8 s^{-1}, 0.2852 g; for SV=2.4 s^{-1}, 0.3696 g)

It is known that the surface coverage of reactants and/or intermediates decreases as the space velocity increases; hence, the activity of the catalyst reduces and also the product distribution may be affected by space velocity depending on the catalyst formulation and the nature of the catalytic reaction (Silva et al., 2007). Figure 4.4 indicates the effect of space velocity on steady state temperature for fresh 2%Pt catalyst. The mean temperature decreased from 112 ^oC to 97 ^oC with the increase of space velocity from 2.4 s^{-1} to 2.8 s^{-1} and then it increased 105 ^oC when the space velocity was further increased to 3.1 s^{-1}. This may indicate the variation of the surface mechanism as a function of the space velocity; i.e. different reaction intermediates form with the space velocity.

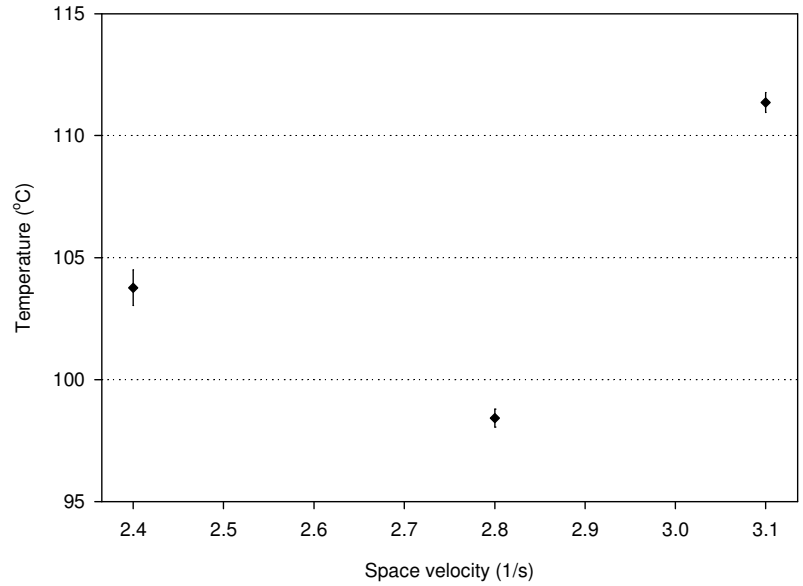

Figure 4.5. Effect of space velocity on steady state temperature for reused catalyst (2% Pt/Al_2O_3, 0.4% CH_3OH, V_T=50 ml/min, T_{in}=28 ^oC, T_{amb}=23 ^oC)

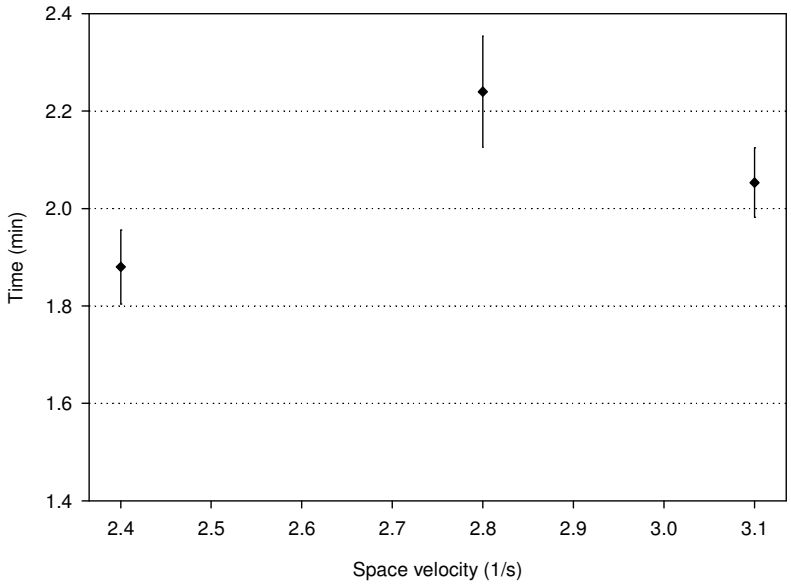

Figure 4.6. Effect of space velocity on time to reach DMFC operation for fresh catalyst (2% Pt/Al_2O_3, 0.4% CH_3OH, V_T=50 ml/min, T_{in}=28 ^oC, T_{amb}=23 ^oC)

Figure 4.5 shows the effect of space velocity on steady state temperature for reused catalyst. This figure also has the same U shape as that seen in Figure 4.4 with the exception of higher steady state temperature being reached at the space velocity of 3.1 s^{-1}. This may be due to the activation procedure that resulted in reduction of surface

PtO_x to Pt; thus, changing the reaction path way in such a way that side blocking "undesirable" intermediates did not form.

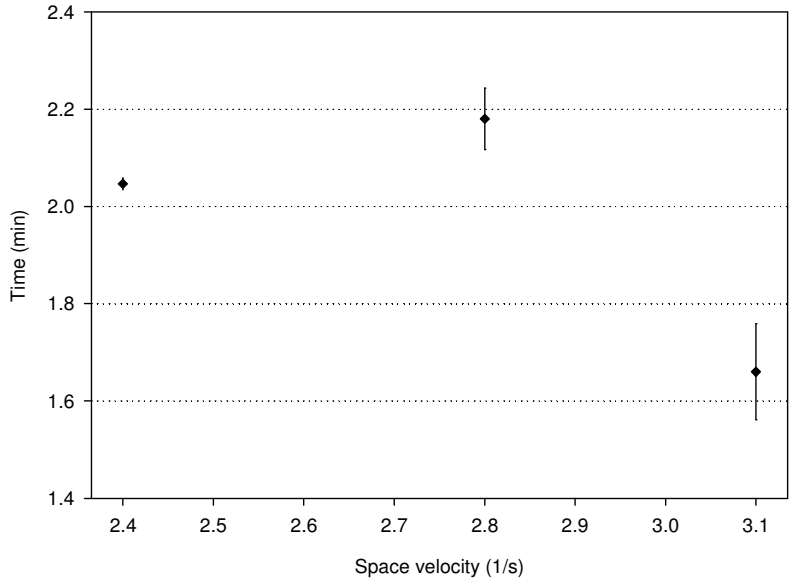

Figure 4.7. Effect of space velocity on time to reach DMFC operation for reused catalyst (2% Pt/Al_2O_3, 0.4% CH_3OH, V_T=50 ml/min, T_{in}=28 ^oC, T_{amb}=23 ^oC)

The effect of space velocity on time to reach DMFC operation temperature for fresh and reused catalysts was shown in Figure 4.6 and 4.7, respectively. Each pattern of Figure 4.6 and 4.7 was dome shape of reaction time to reach at 60 ^oC versus space velocity. Low space velocity (i.e. high residence time) is required to quickly reach at DMFC operating temperature and also to achieve the highest steady state temperature for fresh catalyst whereas high space velocity (i.e. high residence time) is required to quickly reach at DMFC operating temperature and to achieve the highest steady state temperature for reused catalyst.

4.1.3. Effect of Initial Temperature on Methanol Combustion

The fresh and reused 2% Pt/Al_2O_3 catalyst was also tested at the space velocity of 2.4 s^{-1} at 15 ^oC, 7 ^oC and 0 ^oC. It took longer times to reach at steady state for all the sub-room temperatures. While for the initial temperature of 15 ^oC, it took 90 min to reach at steady state, the others reached at steady state temperatures between 90 min and

220 min. The temperature profiles of the sub-room temperatures are listed in Appendix A in Figures A4-A6 and A10-A12.

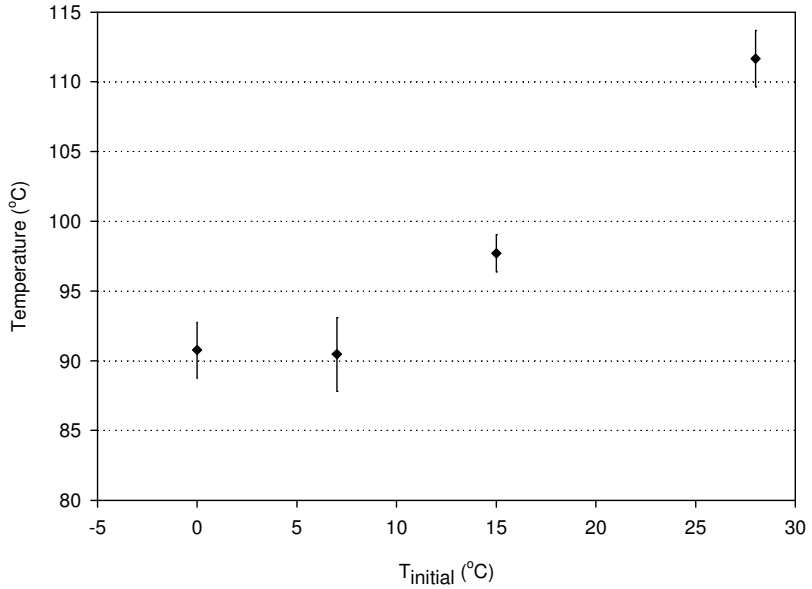

Figure 4.8. Effect of initial temperature on steady state temperature for fresh catalyst (2% Pt/Al_2O_3, 0.4% CH_3OH, V_T=50 ml/min, SV=2.4 s^{-1}, catalyst amount=0.3696 g)

It is known that in general, the quantity of adsorbed molecules on the surface increases as a result of the temperature decrease so the activity of the catalyst reduces. It seems that more methanol or intermediate products adsorbed strongly on much more active sites of the catalyst as the temperature is below the room temperature. Hence, the reaction occurred on the remaining active sites of the surface and the amount of the heat release decreased so that the time to reach steady state increased. The reaction results for the fresh catalyst are given in Figure 4.8.

The mean steady state temperatures are 112 ^oC for the initial temperature of 28 ^oC, 98 ^oC for 15 ^oC and 91 ^oC for 7 and 0 ^oC.

Figure 4.9 shows the effect of initial temperature on steady state temperature for reused catalyst. It was observed that the activation procedure had a significant effect for the initial temperature of 7 ^oC. While there was approximately 6 ^oC reduction for the initial temperature of 28, 15 and 0 ^oC, 6 ^oC increment occurred for 7 ^oC.

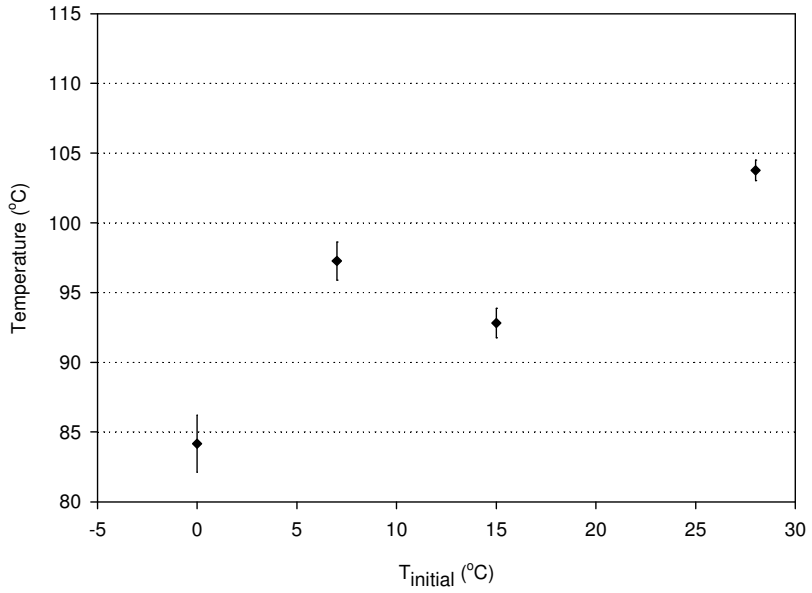

Figure 4.9. Effect of initial temperature on steady state temperature for reused catalyst (2% Pt/Al_2O_3, 0.4% CH_3OH, V_T=50 ml/min, SV=2.4 s^{-1}, catalyst amount=0.3696 g)

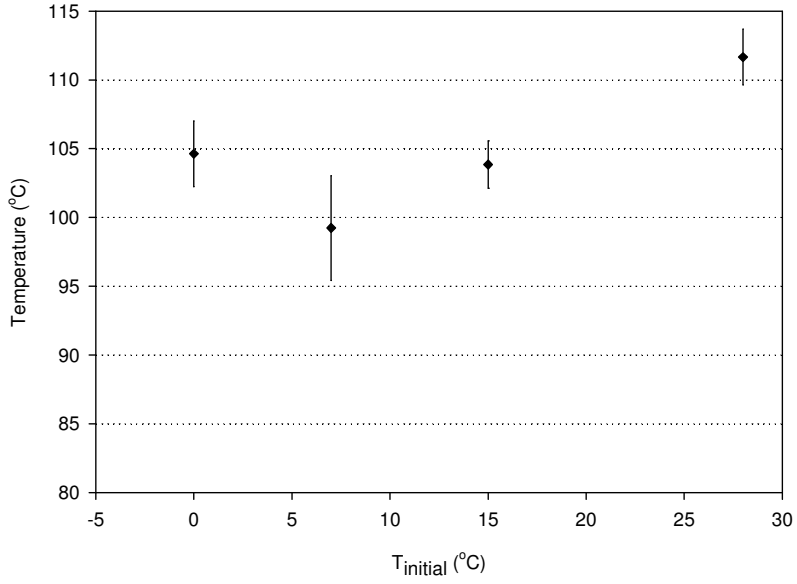

Figure 4.10. Steady state temperatures of the low temperature operations after exposed to the room temperature (2% Pt/Al_2O_3, 0.4% CH_3OH, V_T=50 ml/min, SV=2.4 s^{-1}, catalyst amount=0.3696 g)

After the steady state reaction temperatures were attained, the reactor was exposed to the room temperature while the methanol combustion reaction was continued at room temperature. When the temperatures were at steady state, they were

compared with the reaction temperature of the test occurred at the room temperature (shown in Figure 4.10). It was observed that each of the three reaction temperatures increased and became at steady state at the same temperature within the experimental error. However, they could not reach the steady state temperature of the room temperature test as seen Fig. 4.4. It is possible that the adsorbed reaction by-products at the low temperature did not fully desorb as the outside temperature increases to the room temperature; hence, lowering the original steady state temperature reached when fresh catalyst was first tested at room temperature.

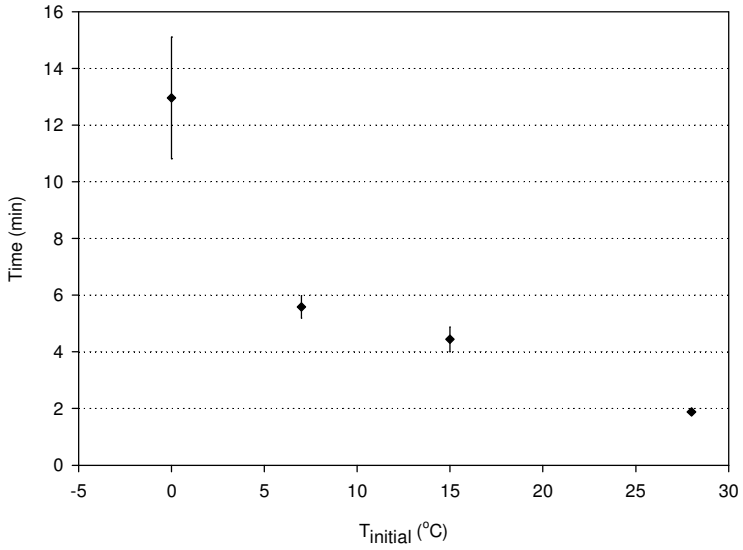

Figure 4.11. Effect of initial temperature on time to reach DMFC operation for fresh catalyst (2% Pt/Al_2O_3, 0.4% CH_3OH, V_T=50 ml/min, SV=2.4 s^{-1}, catalyst amount=0.3696 g)

All the steady state reaction temperatures exceeded the minimum required operating temperature –i.e. 60 ^oC – of DMFC. However, time to reach this temperature is also important. Figure 4.11 and Figure 4.12 indicate the effect of ambient temperature on time to reach 60 ^oC for fresh and reused catalyst, respectively. The time increased as the initial temperature decrease for both cases. It took 10-15 minutes for the initial temperature of 0 ^oC. This was 5 times longer than the other initial temperatures. It seems that the methanol or the reaction intermediates adsorbed strongly on some active sites at 0 ^oC so the temperature increased slowly due to reactions occurring on other sites with relatively less strongly adsorption strength. This is purely speculation and needs to be proven by detailed temperature programmed desorption and reaction techniques.

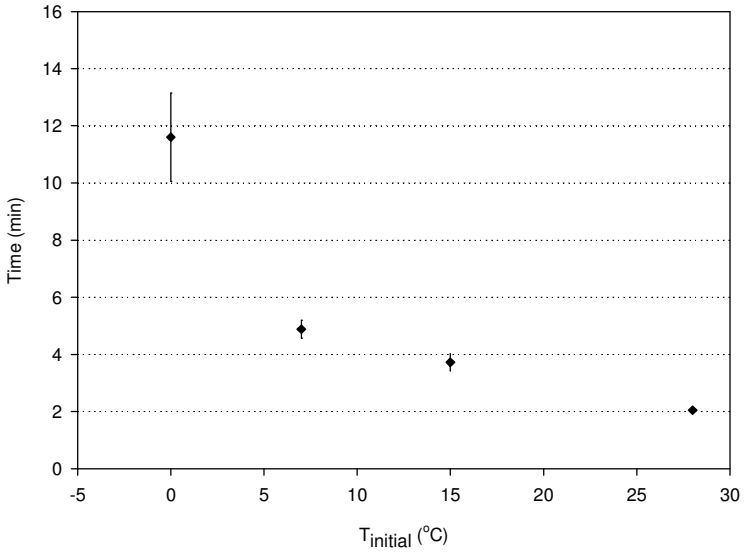

Figure 4.12. Effect of initial temperature on time to reach DMFC operation for reused catalyst (2% Pt/Al_2O_3, 0.4% CH_3OH, V_T=50 ml/min, SV=2.4 s^{-1}, catalyst amount=0.3696 g)

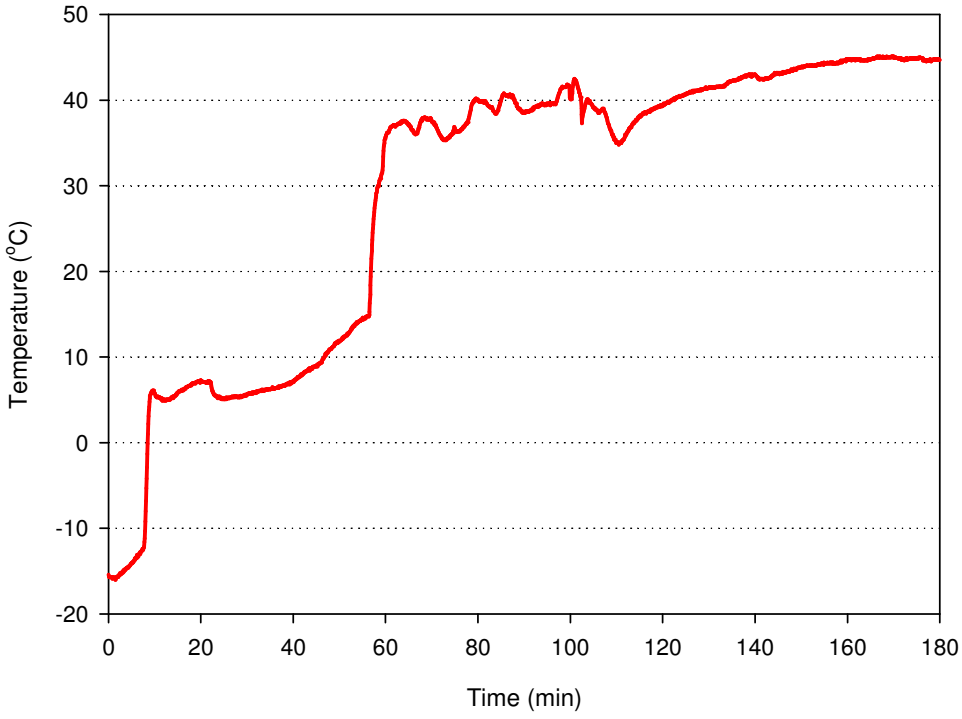

Figure 4.13. Reaction temperature profile for the initial temperature of -15 °C (2% Pt/Al_2O_3, 0.4% CH_3OH, V_T=50 ml/min, SV=2.4 s^{-1}, catalyst amount=0.3696 g)

Figure 4.13 also indicates the reaction temperature profile obtained on 2% Pt/Al_2O_3 for the initial temperature of -15 °C. It took more than 2.5 hour to reach steady

state and the steady state temperature was measured as 45 ^{o}C which is lower than the required operating temperature of the DMFC.

There were sharp increases at the 8 and 57 minutes with 17 and 20 ^{o}C increment, respectively and also, the temperature decreased from 40 ^{o}C to 35 ^{o}C at 122 minute; these fluctuations happened because ice-salt mixture had to be added to the system in order to keep the outside temperature constant at -15 ^{o}C.

4.1.4. Characterization of the Catalysts

Figure 4.14 shows the XRD patterns of the pure and the Pt loaded Al_2O_3 catalysts. All the patterns of Pt/Al_2O_3 catalysts show a diffraction pattern similar to pure γ-Al_2O_3. No diffraction lines associated with Pt was detected so Pt crystallite size was less than 5 nm for all Pt loadings; in other words, platinum was well dispersed on alumina support. This is plausible because it is known that XRD technique is sensitive to the crystallite sizes larger than 5 nm. Moreover, Corro et al. speculated that this small crystallite size may lead to the strong metallic dispersion leading to a homogeneous distribution of the metal atoms on the alumina surface (Corro et al., 2001).

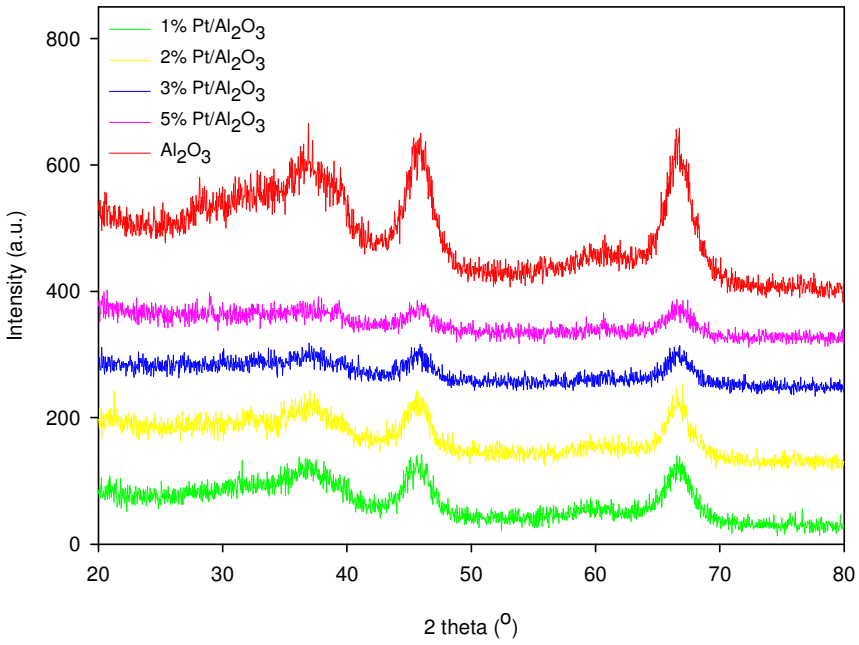

Figure 4.14. XRD pattern of fresh Pt/Al_2O_3 for different loading

After the methanol combustion reaction, 2% and 5% Pt/Al_2O_3 were characterized by XRD and N_2 adsorption analysis in order to observe if there is a change in the particle size.

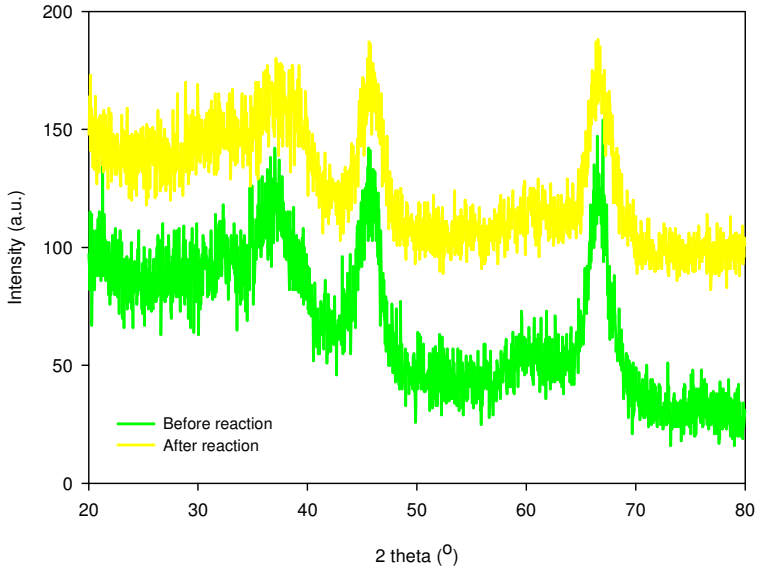

Figure 4.15. XRD pattern of 2% Pt/Al_2O_3 before and after the reactions

The XRD diffraction patterns of 2% and 5% Pt/Al_2O_3 after the methanol combustion reaction for 1 hour are given in Figure 4.15 and Figure 4.16, respectively. There was no obvious change as compared to fresh ones, indicating that Pt particle size in the catalysts did not change during the combustion reaction tests.

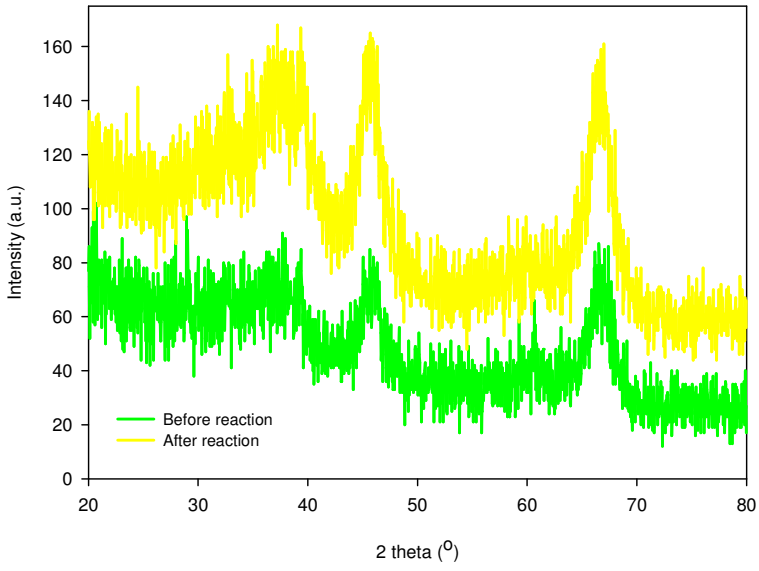

Figure 4.16. XRD pattern of 5% Pt/Al_2O_3 before and after the reactions

However, N_2 adsorption results showed that the surface area for the fresh catalyst was 269 m^2/g, whereas 187 m^2/g for the catalyst after the combustion reactions. This may be due to the adsorbed species left on the catalyst or the local sintering of alumina due to exothermic methanol combustion.

4.2. Plate Coating

After the tests of the methanol combustion reaction on the powder catalysts in the tubular reactor, the reaction was aimed to perform on Pt/Al_2O_3 coated plate reactor because using plate reactor for the methanol combustion is more convenient for DMFC and internal mass transfer limitation and excessive pressure drops can be avoided easily. For this purpose, first of all, Al_2O_3 sol was prepared by sol-gel method at varying concentrations (or viscosity).

After the Al_2O_3 sol preparation at 85 ^oC, the wettability of the Al_2O_3 sol was checked on a stainless steel plate with different viscosities before the coating the plates. Wettability of the sol on the substrate surface should be good for the good coating and contact angle should be smaller than 90 ^{o}. The good wettability is related to the production of OH groups in during the hydrolysis of Al-alkoxide as following reaction (Lee et al., 1993):

$$Al(OR)_3 + 3H_2O \rightarrow Al(OH)_3 + 3ROH \qquad \text{R : Alkyl group} \qquad (4.1)$$

The OH groups bond with the surface of the substrate and the surface coated with the solution.

Figure 4.17 shows the effects of contact angle on the substrate. All the contact angles were smaller than 90^o so the wettability was high and the coating of alumina sol on a stainless steel plate was possible.

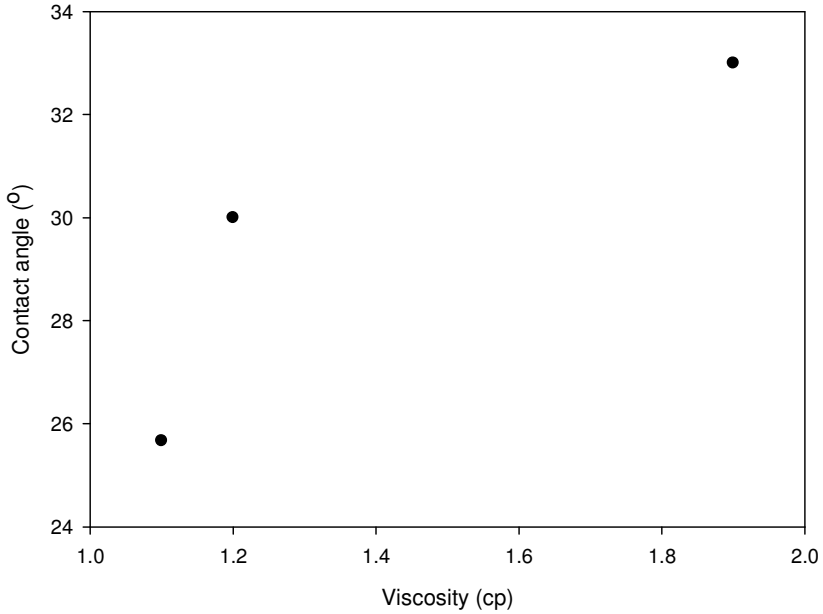

Figure 4.17. Effect of concentration on contact angle for alumina sol on a stainless steel plate

Then, the surfaces of the substrate were cleaned with organic solvents and they were coated with the concentrations of 0.02 g/ml, 0.04 g/ml and 0.07 g/ml Al_2O_3 sol. The concentration was defined as $Al(OH)_3/H_2O$ ratio in this study. The number of coating cycle and the withdrawal speed was 5 and 50 mm/min for each coating, respectively and the plates were waited for 5 min in the sol at the each cycle. After heat treatment, it was observed that the lower concentration sol coatings (0.02 g/ml and 0.04 g/ml) were transparent and brown colored, whereas the 0.07 g/ml Al_2O_3 sol coatings peeled off which is shown in Figure 4.18.

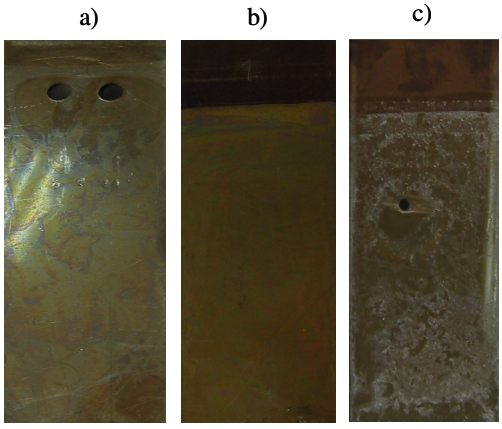

Figure 4.18. Al_2O_3 coated plates after the heat treatment with different concentration (a) 0.02 g/ml, (b) 0.04 g/ml, (c) 0.07 g/ml

Although it was obvious that there was no cracks on the coating of 0.02 g/ml and 0.04 g/ml sols, SEM images were taken to check. Figure 4.19 indicates the SEM micrograph of Al_2O_3 coating on the stainless steel plate. The concentration of the sol was 0.02 g/ml and the number of coating cycle was five. It is seen that there was no crack formation. Thus, it can be said that the good coating can be obtained by the low concentration so the low viscosity sol.

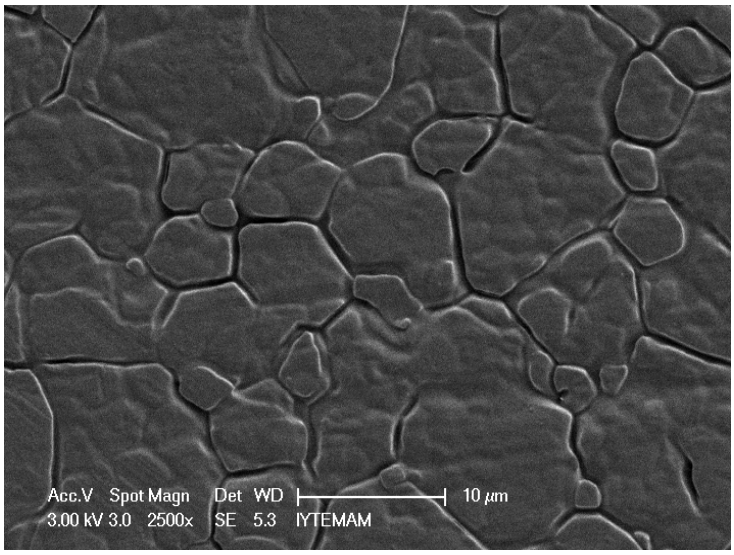

Figure 4.19. SEM micrograph of Al_2O_3 coating on the stainless steel plate

Furthermore, the withdrawal speed of the plate on the weight of Al_2O_3 coating was tested for different concentrations (shown in Figure 4.20). The weight of Al_2O_3 on the substrate is related with the thickness of the coating. Therefore, it is expected that increasing the withdrawal speed increases the thickness so the weight of the Al_2O_3. The coating thickness increases approximately as (withdrawal speed)$^{2/3}$ for the sol-gel processing (Brinker et al., 1990).

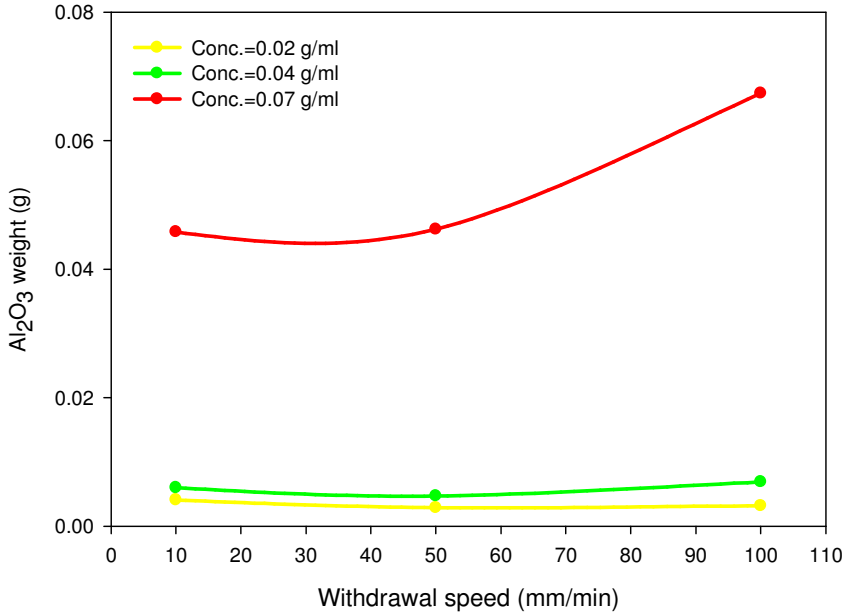

Figure 4.20. Effect of withdrawal speed on the weight of Al_2O_3 coating

It is seen from the Figure 4.20 that the withdrawal speed had a significant effect on the amount of coated Al_2O_3 for the concentration of 0.07 g/ml. The weight of Al_2O_3 on the plate increased dramatically at higher concentration; however, it remained nearly constant for the lower concentrations.

After the preparation of the Al_2O_3 coated plates, it was tried to find the pore volume of the Al_2O_3 for the Pt impregnation. However, it was observed that the pore volume was too small or even no volume. The transparency of the coating was the evident for the absence of the pore volume. The pore volume can be increased either increasing the coating cycle or the direct increasing the surface area by addition of glycerol or PVA to Al_2O_3 sol.

This can be also explained by the BET analyses. While the BET surface area of the pure Al_2O_3 was 242 m^2/g, the Al_2O_3 with glycerol additive was 366 m^2/g. Moreover, adding glycerol reduces crack formation in Al_2O_3 gel (Brinker et al., 1990). In addition to glycerol, one may speculate that the coating did not adhere well on the surface without PVA. PVA also slowed the rate of evaporation of the solvent during heat treatment and prevented crack formation on the Al_2O_3 coated surface that would have been caused by fast evaporation (Agrafiotis et al., 2002).

The surface areas of boehmite gels are quite sensitive to the H_2O/Al ratio used in the gel synthesis procedure. Reduction of the H_2O/Al ratio increases the surface area of

the boehmite gels so the porosity (Brinker et al., 1990). Therefore, Al_2O_3 sol prepared at higher concentrations of 0.09 g/ml and 0.12 g/ml additional to 0.07 g/ml with glycerol and PVA additive.

The Al_2O_3 sols with additives were coated on the substrates once with the withdrawal speed of 10 mm/min. The amount of Al_2O_3 on the substrate increased with the concentration increase as shown in Figure 4.21. This was consistent with the previous results.

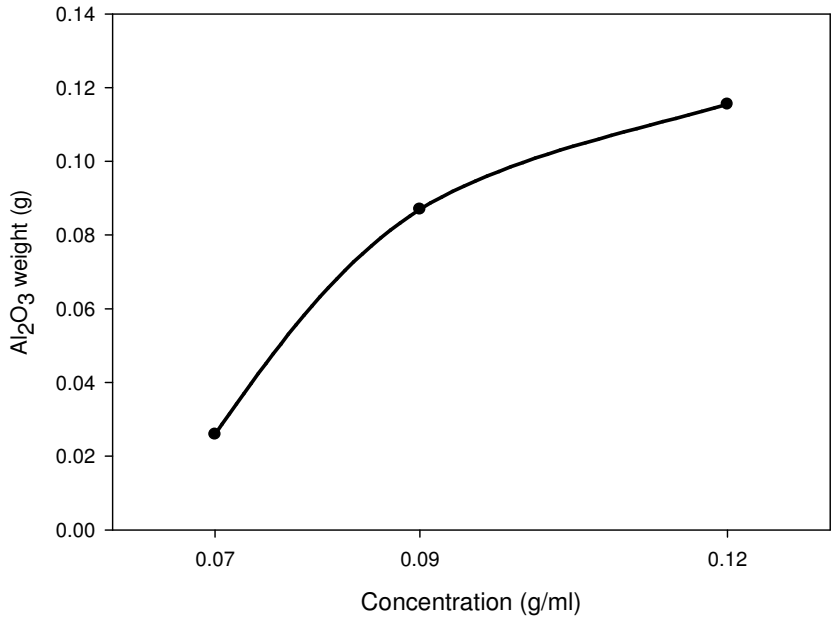

Figure 4.21. Effect of concentration on the weight of Al_2O_3 coating after adding 2% wt. glycerol to the sol

Furthermore, it was observed that the additive type had a significant effect on the coating amount. Sols with the concentration of 0.12 g/ml with 1% wt. glycerol and 1% wt. PVA were prepared and they were coated on the substrates keeping the other parameters (coating cycle, withdrawal speed, etc.) constant. The weight of Al_2O_3 with glycerol additive (0.032 g) on the substrates was two times higher than the Al_2O_3 with PVA additive (0.016 g).

However, crack formation and peeling offs were observed on all the coated plates. The occurrence of cracks with increasing concentration (or viscosity) may be caused by the reduction of OH group which is required for bonding with the substrate in accordance with the hydrolysis and polycondensation reactions (Lee et al., 1993).

The pore volume of the coating could not be measured because of the cracks and peeling offs so Pt could not be impregnated on the Al_2O_3. Further studies are necessary to prevent the crack formation and to increase the porosity.

CHAPTER 5

CONCLUSION

In this study, the effect of the platinum loading, space velocity and the outside temperature on the activity of the Pt/Al_2O_3 catalysts in the methanol combustion was investigated.

It was observed that there were 3 ^oC increments in temperature on the pure alumina as the feed mixture was fed to the reactor and then, the temperature decreased to the initial reactor temperature. This may be due to either the adsorption or dehydration of the methanol on the Al_2O_3 surface. However, Pt/Al_2O_3 catalysts with varying loadings were active in methanol combustion starting at room temperature.

There was a significant difference in the steady state temperatures between 1% and 5% Pt catalysts. However, 2, 3 and 5% Pt loading catalysts had nearly the same temperature and they reached at 60 ^oC at the same time. Hence, it seems that the average crystallite size and the crystallite size distribution of Pt on 2, 3 and 5% Pt loading catalysts would be similar, but that of 1% Pt/Al_2O_3 would be different from the other catalysts.

Three different space velocities with 15% increment (2.4 s^{-1}, 2.8 s^{-1} and 3.1 s^{-1}) were tested on fresh and reused 2% Pt/Al_2O_3 catalyst. At the first %15 increment of the space velocity, the steady state temperature of fresh catalyst decreased, but the further increase in the space velocity increased the temperature. This may be explained by the variation of the surface mechanism as a function of the space velocity. On the other hand, the steady state temperature of reused catalyst at 3.1 s^{-1} increased higher than the steady state temperature of fresh catalyst. This may be resulted from the activation procedure.

Moreover, it was observed that the activity of the catalysts decreased as the outside temperature decrease due to the stronger adsorption of the reactants or the reaction by-products on the surface with outside temperature decrease except for the initial temperature of 7 ^oC for reused catalyst. It was seen that the activation procedure had a significant effect on the activity of this catalyst at this temperature. The steady state reaction temperatures exceeded the temperature of 60 ^oC at all the sub-room

temperatures and the time to reach this temperature increased as the initial temperature decrease.

After the steady state reaction temperatures were attained, the reactor was exposed to the room temperature from the sub-room temperatures (0 ^{o}C, 7 ^{o}C, 15 ^{o}C). It was found that the reaction temperatures of the all catalysts increased and they were all at steady state at the same temperature in 15 minutes but the temperatures were below the room temperature test. It can be said that the adsorbed reaction by-products at the low temperature did not fully desorb.

In addition to these temperatures, the activity of the catalyst was also tested at the initial temperature of -15 ^{o}C. It was observed that the catalyst was still active at that temperature, however, it could not reach the required operating temperature of the DMFC within 120 min of the reaction time; therefore, the space velocity might be increased in order to quickly reach the required temperature.

After the activity tests, the XRD results showed that Pt particle size in the catalysts did not change, however, BET analyses indicated that the surface area of the fresh catalyst decreased after the reactions. This may be due to the adsorbed species left on the catalyst or the local sintering of alumina due to exothermic methanol combustion.

Furthermore, the plate reactor was tried to prepare the catalysts coated on the stainless steel plates for the methanol combustion because it is more suitable for use in the DMFC than the tubular reactor. However, the appropriate thickness could not be obtained due to the excessive crack formation and peeling off; therefore, further studies are necessary to find the optimal thickness.

REFERENCES

Agrafiotis C, Tsetsekou A., 2002, "Depostion of meso-porous γ-alumina coatings on ceramic honeycombs by sol–gel methods", Journal of the European Ceramic Society, Vol. 22, pp. 423–34

Álvarez-Galván M.C., Pawelec B., Peña O'Shea V.A., Fierro J.L.G, Arias P.L., 2004, "Formaldehyde/methanol combustion on alumina-supported manganese-palladium oxide catalyst", Applied Catalysis B: Environmental, Vol. 51, pp. 83–91

Arnby K., Törncrona A., Skoglundh M., 2004, "Influence of ammonia on CO and methanol oxidation over $Pt/\gamma\text{-}Al_2O_3$ catalysts modified by Mg", Applied Catalysis B: Environmental, Vol. 49, pp. 51–59

Avcı A.K., Trimm D.L., Karakaya M., 2010, "Microreactor catalytic combustion for chemicals processing", Catalysis Today, Vol. 155, pp. 66–74

Badlani M., Wachs I.E., 2001, "Methanol: a "smart" chemical probe molecule", Catalysis Letters, Vol. 75, No. 3–4

Basu, S, 2007, "Future Directions of Fuel Cell Science and Technology", Recent Trends in Fuel Cell Science and Technology, pp. 356-365

Bond G., Thompson D. T., 1999, "Catalysis by Gold", Catalysis Reviews, Science and Engineering, Vol. 41, pp. 319–388

Brinker C.F., Scherer G.W., 1990, "Sol-Gel Science", Academic Press, Inc., pp. 788-790

Cao C., Hohn K. L., 2009, "Study of reaction intermediates of methanol decomposition and catalytic partial oxidation on Pt/Al_2O_3", Applied Catalysis A: General, Vol. 354, pp. 26–32

Chantaravitoon P., Chavadej S., Schwank J., 2004, "Temperature-programmed desorption of methanol and oxidation of methanol on $Pt–Sn/Al_2O_3$ catalysts", Chemical Engineering Journal, Vol. 97, pp. 161–171

Corro G., Aguilar G., Montiel R., Bernes S., 2001, "Method For Metal Dispersion Measurements on $Pt\text{-}Sn/\gamma\text{-}Al_2O_3$", Reaction Kinetics and Catalysis Letters, Vol. 73, No. 2, pp. 317-323

Croy J. R., Mostafa S., Liu J., Sohn Y., Heinrich H., Cuenya B. R., 2007, "Support Dependence of MeOH Decomposition Over Size-Selected Pt Nanoparticles", Catalysis Letters, Vol. 119, pp. 209–216

Fernandez-Pello A.C., 2002, "Micropower Generation Using Combustion: Issues and Approaches", Proceedings of the Combustion Institute, Vol. 29, pp. 883–899

Ferrin P., Mavrikakis M., 2009, "Structure Sensitivity of Methanol Electrooxidation on Transition Metals", Journal of the American Chemical Society, Vol. 131, No. 40, pp. 14381–14389

Fuel Cells, April 2008, US Industry Study with Forecasts for 2012 & 2017

Fuel cells, 2009, "Fuel Cell Basics", The Online Fuel Cell Information Resource, August 28, from http://www.fuelcells.org/basics/benefits.html

Eastmidlands, 2009, "Natural Gas", Groundwork Leicester & Leicestershire, July 16, from http://www.eastmidlands.groundwork.org.uk/leicester--leicestershire.aspx

Energy Information Administration Office of Integrated Analysis and Forecasting U.S. Department of Energy, May 2009, International Energy Outlook

Energy Information Administration Office of Integrated Analysis and Forecasting U.S. Department of Energy, August 2009, International Energy Data and Analysis for Turkey

Energy Policies of IEA Countries, Turkey, 2005, International Energy Agency

Gates, B.C., Katzer, J.R., Schuit G.C.A., 1979, "Chemistry of Catalytic Processes", McGraw-Hill: New York, pp. 325-388

Hinz A., Larsson P., Andersson A., 2002, "Influence of Pt loading on Al_2O_3 for the low temperature combustion of methanol with and without a trace amount of ammonia", Catalysis Letters, Vol. 78, No. 1–4

Iea, 2009, "Renewable Energy", International Energy Agency, July 24, from http://www.iea.org/

Iupap, 2009, "Fuel Cells", International Union of Pure and Applied Physics (IUPAP) Energy Reports, August 15, from http://www.iupap.org/wg/energy/annexv.pdf

Jensen K.F., 2001, "Microreaction engineering is small better?", Chemical Engineering Science, Vol. 56, pp. 293-303

Jin J., Kwon S., 2010, "Fabrication and performance test of catalytic micro-combustors as a heat source of methanol steam reformer", International Journal of Hydrogen Energy, Vol. 35, pp. 1803-1811

Kakaç S., Pramuanjaroenkij A., Vasiliev L., 2008, "Mini-Micro Fuel Cells: Fundamentals and Applications", Netherlands, Springer

Lee J. W, Won C. W., Chun B. S., Sohn H. Y., 1993, "Dip coating of alumina films by the sol-gel method", Journal of Materials Research**,** Vol. 8, No. 12, pp. 3151-3157

Lee E.Y., Park Y.K., Joo O.S, Jung K.D., 2006, "Methanol Dehydration to Produce Dimethyl Ether Over γ-Al_2O_3", Reaction Kinetics and Catalysis Letters, Vol. 89, No. 1, pp. 115-121

Lee J.S., Han S.H., Kim H.G., Lee K.H., Kim G.L., 2000, "Effects of Space Velocity on Methanol Synthesis from $CO_2/CO/H_2$ over $Cu/ZnO/Al_2O_3$ Catalyst", Korean Journal of Chemical Engineering, Vol. 17, No. 3, pp. 332-336

Leu C.H., King S.C., Chen C.C., Huang J.M., Tzeng S.S, Liu I.H, Chang W.C, 2010, "Investigation of the packed bed and the micro-channel bed for methanol catalytic combustion over $Pt/A1_2O_3$ catalysts", Applied Catalysis A: General, Vol. 382, pp. 43–48

Lippits M.J., Boer Iwema R.R.H., Nieuwenhuys B.E., 2009, "A comparative study of oxidation of methanol on γ-Al_2O_3 supported group IB metal catalysts", Catalysis Today, Vol. 145, pp. 27–33

Ma Y., Ricciuti C., Miller T., Kadlowec J., Pearlman H., 2008, "Enhanced Catalytic Combustion Using Sub-micrometer and Nano-size Platinum Particles", Energy & Fuels, Vol. 22, pp. 3695–3700

Mam, 2009, "Fuel Cells", Tübitak Marmara Araştırma Merkezi, September 2, from http://www.mam.gov.tr

Minicò S., Scirè S., Crisafulli C., Maggiore R., Galvagno S., 2000, "Catalytic combustion of volatile organic compounds on gold/iron oxide catalysts", Applied Catalysis B: Environmental, Vol. 28, pp. 245–251

Mmoistanbul, 2009, "Fuel Cells", İstanbul Büyükşehir Belediyesi, August 28, from http://www.mmoistanbul.org

Nakagawa N., Xiu Y., 2003, "Performance of a direct methanol fuel cell operated at atmospheric pressure", Journal of Power Sources, Vol. 118, pp. 248–255

Nishibori M., Shin W., Tajima K., Houlet L.F., Izu N., Itoh T., Matsubara I., 2008, "Long-term stability of Pt/alumina catalyst combustors for micro-gas sensor application", Journal of the European Ceramic Society 28 (2008) 2183–2190

Nuhu A., Soares J., Gonzalez-Herrera M., Watts A., Hussein G., Bowker M., 2007, "Methanol oxidation on Au/TiO_2 catalysts", Topics in Catalysis, Vol. 44, Nos. 1–2

Prasad, R., Kennedy, L. A., Ruckenstein E., 1984, "Catalytic Combustion", Catalysis Reviews, Science and Engineering, Vol. 26, No. 1, pp. 1-58

Report of Hard Coal Sector, May 2009, General Management of Turkish Hard-coal Enterprises

Ryi S.K., Park J.S, Choi S.H., Cho S.H., Kim S.H., 2005. "Novel micro fuel processor for PEMFCs with heat generation by catalytic combustion", Chemical Engineering Journal, Vol. 113, pp. 47–53

Schiffimo R.S., Merrill R.P., 1993, "A Mechanistic Study of the Methanol Dehydration Reaction on γ-Alumina Catalyst", The Journal of Physical Chemistry, Vol. 97, pp. 6425-6435

Shanna D. Knights, Kevin M. Colbow, Jean St-Pierre, David P. Wilkinson, 2004, "Aging mechanisms and lifetime of PEFC and DMFC", Journal of Power Sources, Vol. 127, pp. 127–134

Sharma R. K., Zhou B., Tong S., Chuan K. T., 1995, "Catalytic Destruction of Volatile Organic Compounds Using Supported Platinum and Palladium Hydrophobic Catalysts", Industrial & Engineering Chemistry Research, Vol. 34, pp. 4310-4317

Shah R.K., 2007, "Introduction to Fuel Cells", Recent Trends in Fuel Cell Science and Technology, pp. 1-9

Silva F.A., Martinez D.S., Ruiz J.A.C, Mattos L.V, Noronha F.B., Horia C.E., 2007, "The Effect of Pt Loading and Space Velocity on the Performance of $Pt/CeZrO_2/Al_2O_3$ Catalysts for the Partial Oxidation of Methane", Natural Gas Conversion VIII, Vol. 167, pp. 427-432

Spivey J.J., 1987, "Complete Catalytic Oxidation of Volatile Organics", Industrial & Engineering Chemistry Research, Vol. 26, pp. 2165-2180

Spivey J. J., Roberts G. W., 2004, "Catalysis", The Royal Society of Chemistry Vol. 17, p.p. 1-115

The engineering tool box, 2009, “Material Properties”, Resources, Tools and Basic Information for Engineering and Design of Technical Applications, August 18, from http://www.engineeringtoolbox.com/

Urban P.M., Funke A., M¨uller J.T., Himmen M., Docter A., 2001, “Catalytic processes in solid polymer electrolyte fuel cell systems”, Applied Catalysis A: General, Vol. 221, pp. 459–470

World Energy Council Turkish National Committee, December 2007, 2005-2006 Energy Report of Turkey

World Energy Outlook, 2008, International Energy Agency

World Fuel Cells, May 2009, Industry Study with Forecasts for 2013 & 2018

Xu K., Pierce D. T., Li A., Zhao J. X., 2008, “Nanocatalysts in Direct Methanol Fuel Cell Applications”, Synthesis and Reactivity in Inorganic, Metal-Organic, and Nano-Metal Chemistry, Vol. 38, pp. 394–399

APPENDIX A

REACTION TEMPERATURE PROFILES

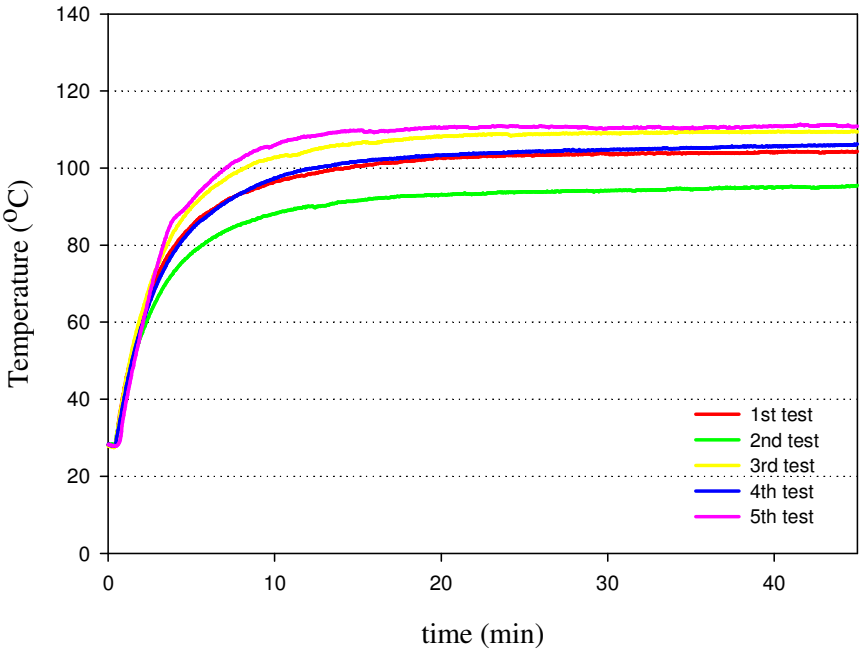

Figure A.1. Temperature profile of 2% Pt/Al_2O_3 fresh catalysts at the space velocity of 3.1 s^{-1} (0.4 % CH_3OH, V_T=50 ml/min, T_{in}=28 °C, T_{amb}=20 °C, catalyst amount=0.2008 g)

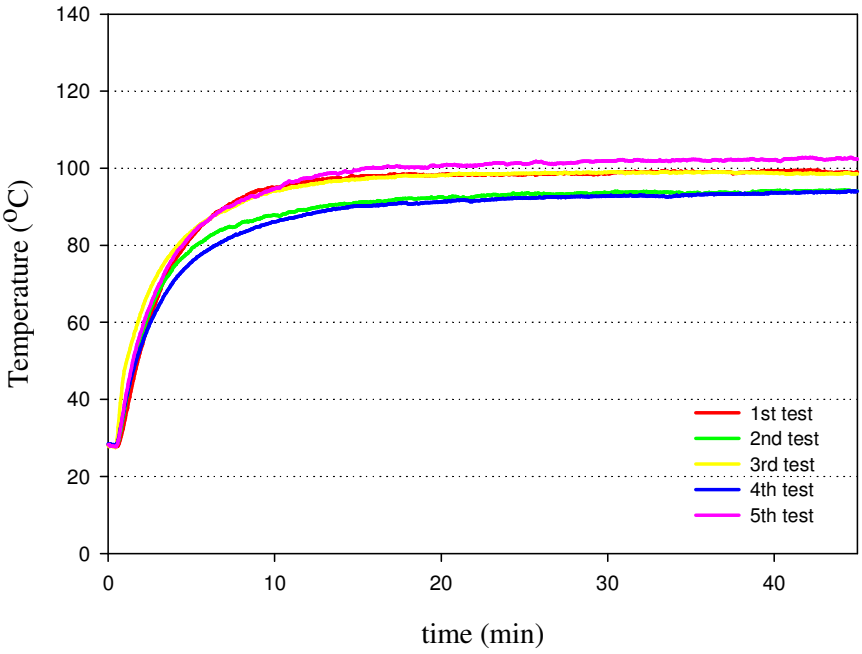

Figure A.2. Temperature profile of 2% Pt/Al_2O_3 fresh catalysts at the space velocity of 2.8 s^{-1} (0.4 % CH_3OH, V_T=50 ml/min, T_{in}=28 °C, T_{amb}=22 °C catalyst amount=0.2852 g)

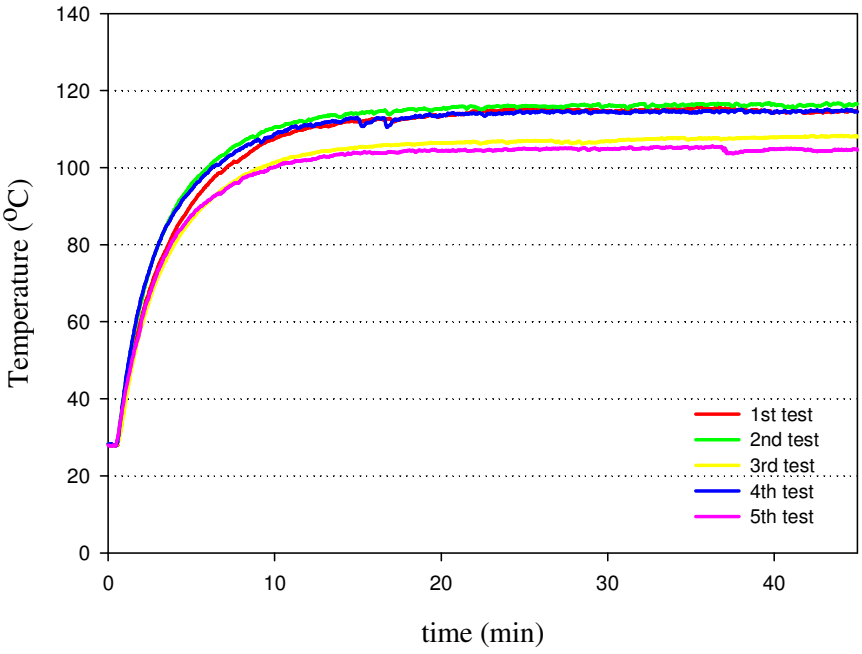

Figure A.3. Temperature profile of 2% Pt/Al_2O_3 fresh catalysts at the space velocity of 2.4 s^{-1} (0.4 % CH_3OH, V_T=50 ml/min, T_{in}=28 °C, T_{amb}=23 °C catalyst amount=0.3696 g)

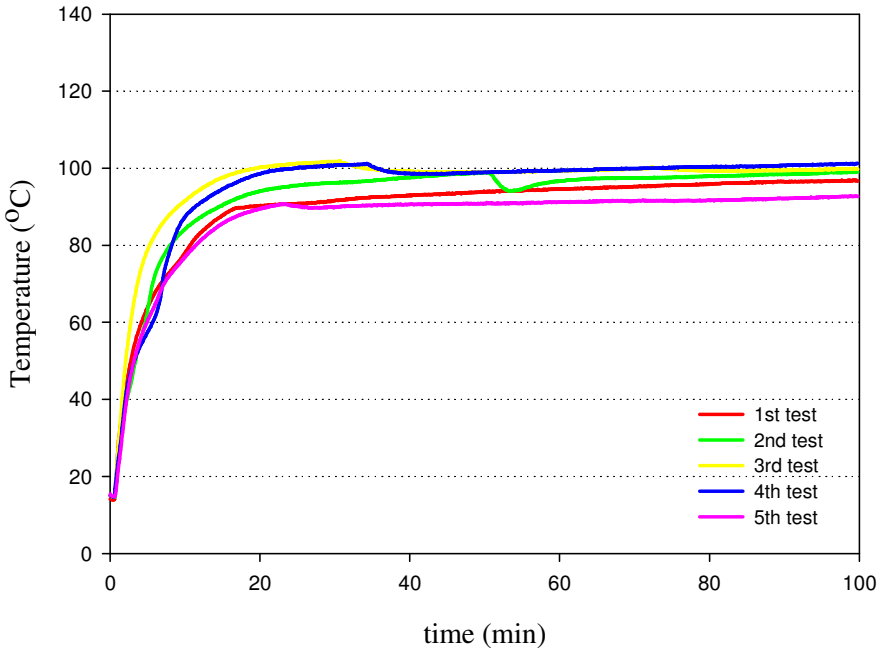

Figure A.4. Temperature profile of 2% Pt/Al_2O_3 fresh catalysts at the initial temperature of 15 °C (0.4 % CH_3OH, V_T=50 ml/min, T_{amb}=10 °C, SV=2.4 s^{-1} catalyst amount=0.3696 g)

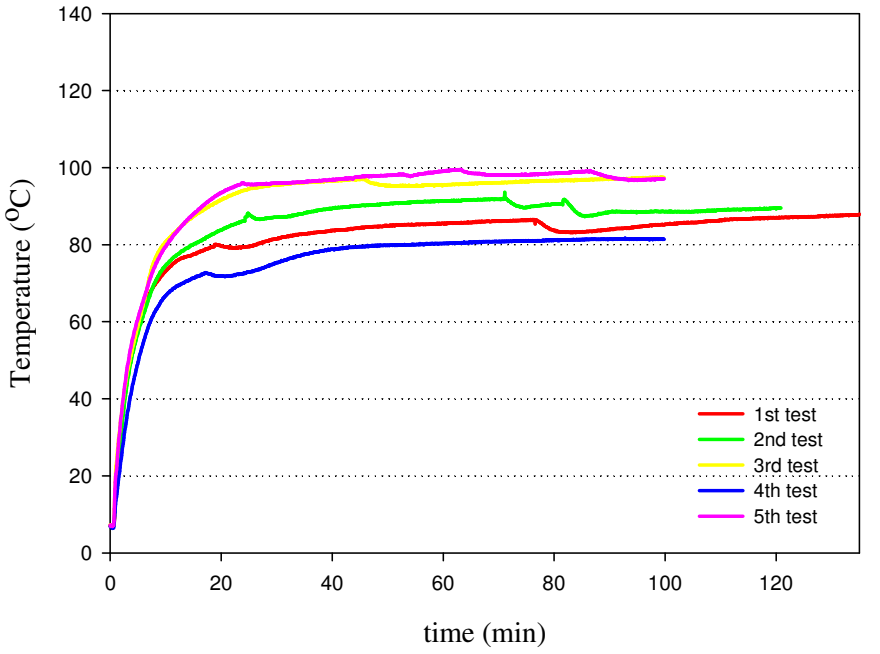

Figure A.5. Temperature profile of 2% Pt/Al_2O_3 fresh catalysts at the initial temperature of 7 °C (0.4 % CH_3OH, V_T=50 ml/min, T_{amb}=2 °C, SV=2.4 s^{-1} catalyst amount=0.3696 g)

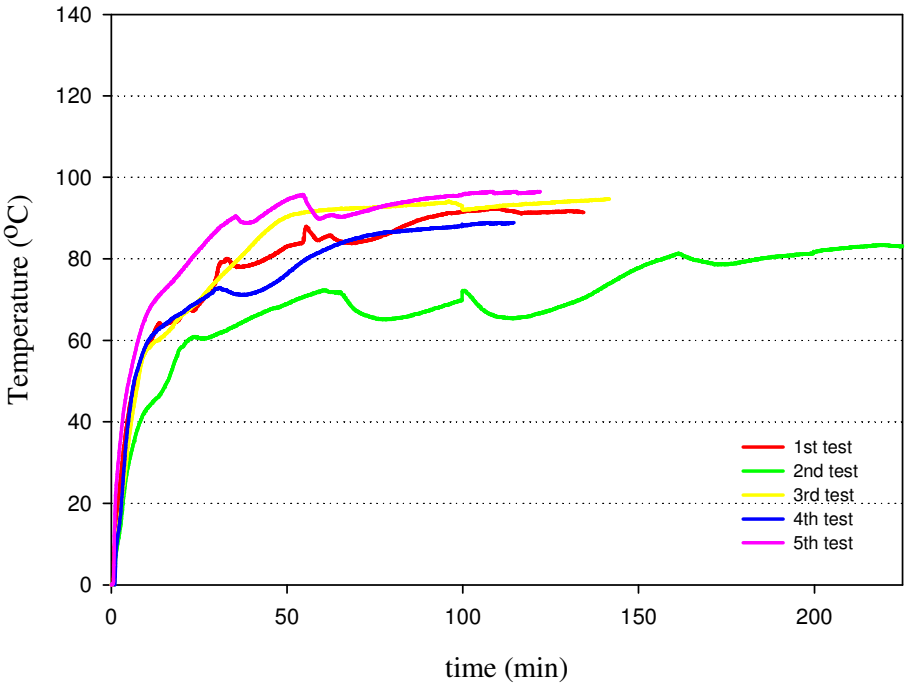

Figure A.6. Temperature profile of 2% Pt/Al_2O_3 fresh catalysts at the initial temperature of 0 °C (0.4 % CH_3OH, V_T=50 ml/min, T_{amb}= -5 °C, SV=2.4 s^{-1}, catalyst amount=0.3696 g)

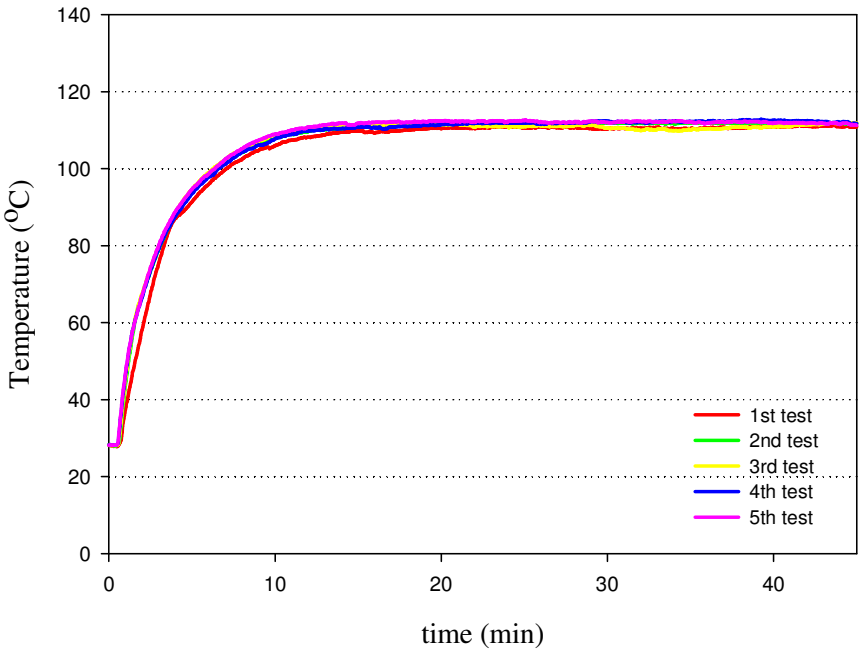

Figure A.7. Temperature profile of 2% Pt/Al_2O_3 reused catalysts at the space velocity of 3.1 s^{-1} (0.4 % CH_3OH, V_T=50 ml/min, T_{in}=28 °C, T_{amb}=24 °C, catalyst amount=0.2008 g)

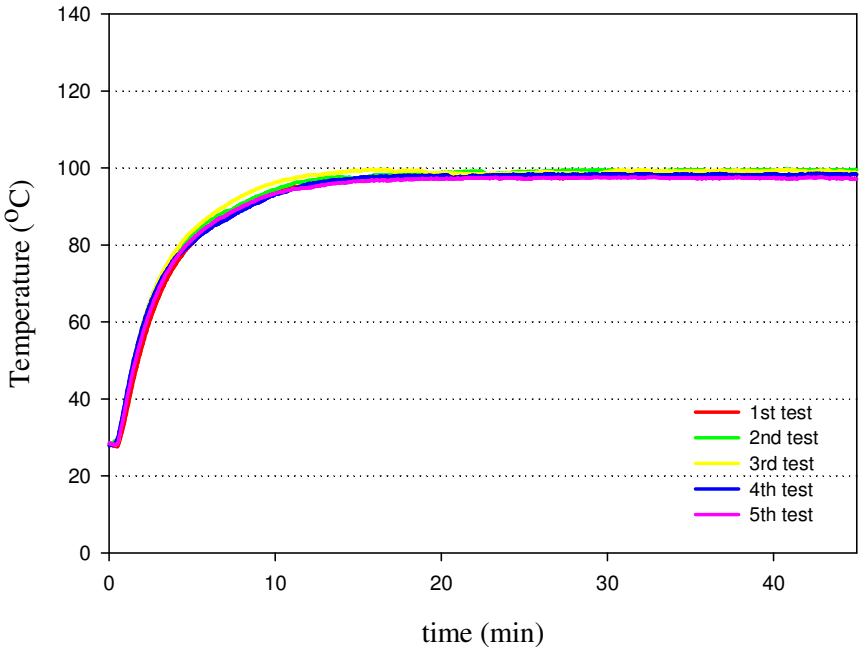

Figure A.8. Temperature profile of 2% Pt/Al_2O_3 reused catalysts at the space velocity of 2.8 s^{-1} (0.4 % CH_3OH, V_T=50 ml/min, T_{in}=28 °C, T_{amb}=23 °C, catalyst amount=0.2852 g)

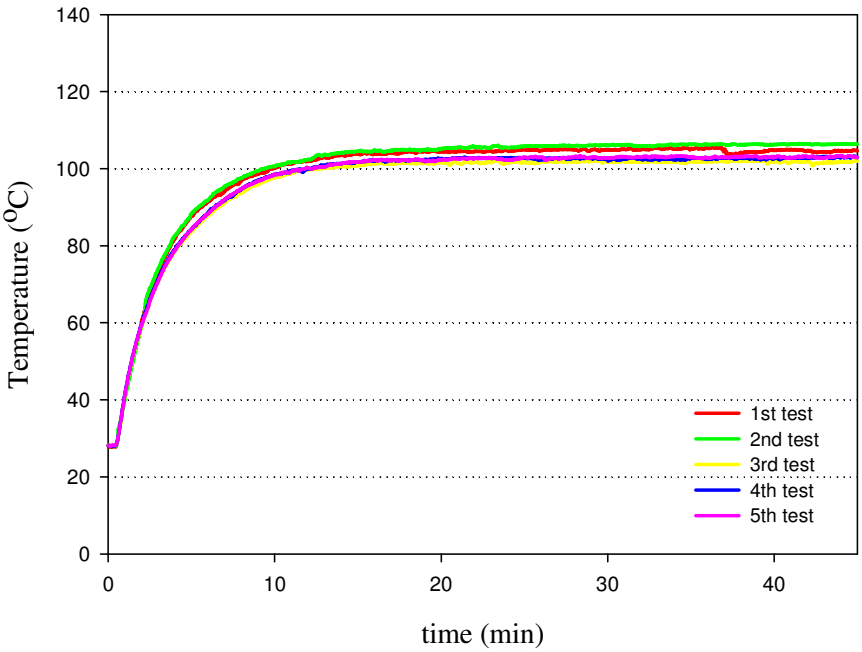

Figure A.9. Temperature profile of 2% Pt/Al_2O_3 reused catalysts at the space velocity of 2.4 s^{-1} (0.4 % CH_3OH, V_T=50 ml/min, T_{in}=28 °C, T_{amb}=23 °C, catalyst amount=0.3696 g)

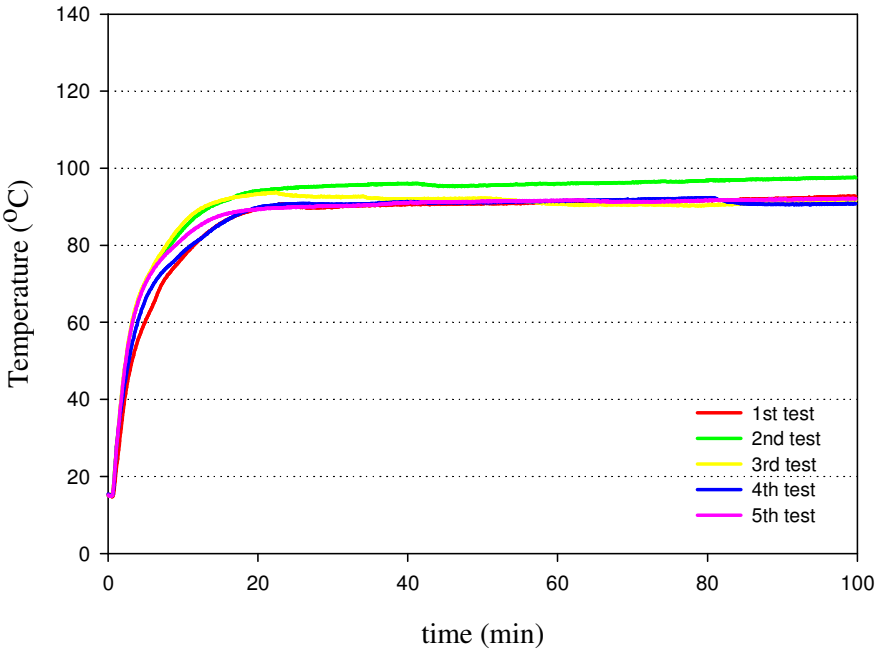

Figure A.10. Temperature profile of 2% Pt/Al_2O_3 reused catalysts at the initial temperature of 15 °C (0.4 % CH_3OH, V_T=50 ml/min, T_{amb}=10 °C, SV=2.4 s^{-1}, catalyst amount=0.3696 g)

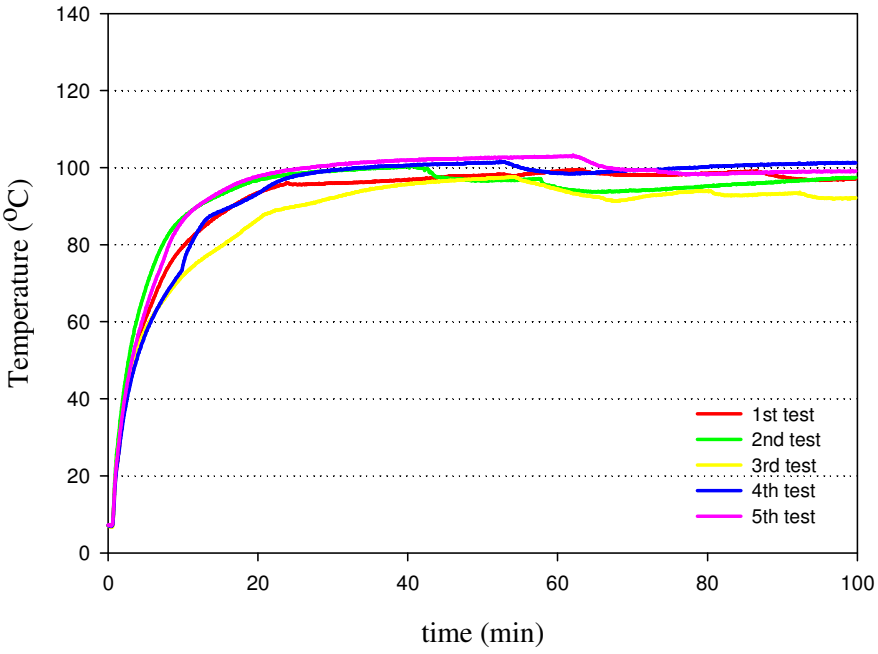

Figure A.11. Temperature profile of 2% Pt/Al_2O_3 reused catalysts at the initial temperature of 7 °C (0.4 % CH_3OH, V_T=50 ml/min, T_{amb}=2 °C, SV=2.4 s^{-1}, catalyst amount=0.3696 g)

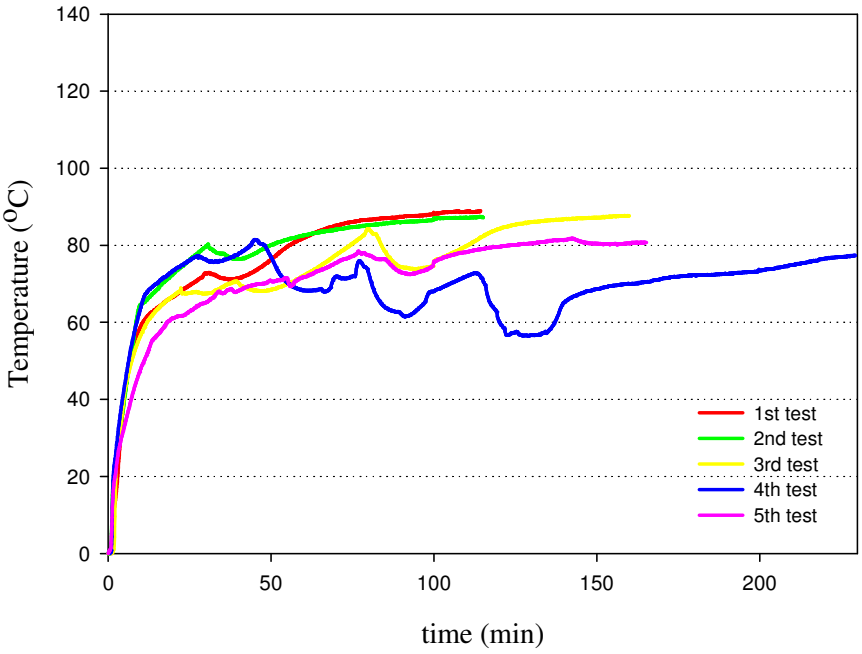

Figure A.12. Temperature profile of 2% Pt/Al_2O_3 reused catalysts at the initial temperature of 0 ^{o}C (0.4 % CH_3OH, V_T=50 ml/min, T_{amb}= -5 ^{o}C, SV=2.4 s^{-1}, catalyst amount=0.3696 g)

APPENDIX B

ADIABATIC FLAME TEMPERATURE CALCULATION

The inlet and the outlet streams of the methanol combustion were shown in Figure B.1.

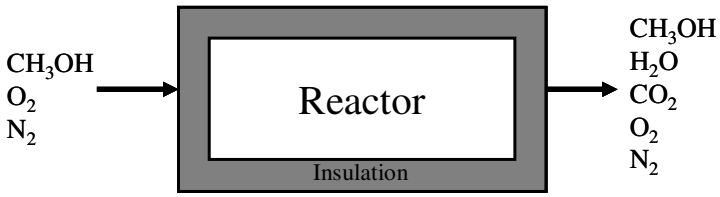

Figure B.1. Reactants and the products of the methanol combustion

Overall steady state energy balance for flow systems is;

$$\dot{Q}+\dot{W}+\sum \dot{N}_{i_0} H_{i0} - \sum \dot{N}_i H_i = 0 \qquad \text{(B.1)}$$

The assumptions are;

- The system is at steady state.
- The reactor was insulated so no heat is lost to the surrounding ($Q = 0$).
- No work is produced ($W = 0$).

So the energy balance around the reactor is;

$$\sum \dot{N}_{i_0} H_{i0} - \sum \dot{N}_i H_i = 0 \qquad \text{(B.2)}$$

Since the heat capacities changes with temperature, the equation to calculate the adiabatic flame temperature is;

$$\dot{N}_{A_0} \sum_{i=1}^{n} \int_{T_{in}}^{T_{ad}} \Theta_i Cp_i dT - \left[\Delta H^\circ_{Rxn}(T_R) + \int_{T_R}^{T_{ad}} \Delta Cp_j dT \right] \dot{N}_{A_0} X_A = 0 \qquad \text{(B.3)}$$

The heat capacities were calculated by using the equation of B.4. The heat of reactions (at 298 K and 1 atm) and the heat capacity constants were given in Table B.1.

$$Cp = a + bT + cT^2 + dT^4 + eT^5 \quad \text{(B.4)}$$

Table B.1. Heat of reactions and the heat capacity constants
(Source: The engineering tool box, 2009)

Species	ΔH°_{Rxn} (kJ/kmol)	Heat capacity constants				
		a	b	c	d	e
CH_3OH	-201000	21.152	0.07092	2.59E-05	-2.85E-08	0
O_2	0	0.8587	8.17E-05	5.02E-07	-4.80E-10	1.28E-13
N_2	0	1.1095	-5.18E-04	1.15E-06	-7.35E-10	1.57E-13
CO_2	-393500	0.50222	1.39E-03	-8.51E-07	1.92E-10	0
H_2O	-241820	1.785	8.29E-05	6.29E-07	-2.11E-10	0

The adiabatic flame temperature was calculated using the equation of B.3 for a given methanol conversion.